Gutierrez *et al.*
Environmental Sciences Europe (2025) 37:67
https://doi.org/10.1186/s12302-025-01084-y

Environmental Sciences Europe

RESEARCH

Open Access

Geospatial physiologically based demographic modeling and analysis of thirteen invasive species in Africa: why the biology matters

Andrew Paul Gutierrez[1,2*], Luigi Ponti[1,3], Markus Neteler[1,4], Federica Stocchino[5], Jose Ricardo Cure[1,6], Peter E. Kenmore[1] and George Simmons[7]

Abstract

Background Globally, research and policy groups often lack the expertise to develop models to analyze invasive and native species of agroecological and veterinary/human health importance; models to inform management and policy under extant and climate change scenarios at various geographic scales. Species distribution models (SDMs) correlate weather and other variables to species presence records and are currently the mainstay for predicting the geographic distribution of species, but SDMs do not predict the underpinning dynamics required to develop policy and management strategies. Weather-driven physiologically based demographic models (PBDMs) of single and multi-trophic dynamics based on sound biological data can bridge much of this gap. The development of web platform software is proposed to assist non-experts in formulating PBDMs to help solve agroecological and veterinary/human health pest problems.

Results PBDMs are time-varying life tables (TVLTs) that capture the weather-driven biology of per capita resource acquisition and allocation to growth and reproduction in age-mass structured trophic settings independent of time and place. Two approaches are used to parameterize PBDMs: (1) mass/energy acquisition and allocation, and (2) biodemographic functions fitted to vital rates estimated from age-specific life table studies conducted under a range of abiotic conditions; vital rates that result from resource acquisition and allocation under experimental conditions. To outline the development and demonstrate the utility of this approach as web platform software for nonexperts, PBDMs for thirteen species of agroecological and medical/veterinary importance to Africa are developed and used to predict prospectively their geographic distribution, relative abundance, and dynamics across the continent. Where possible, PBDM predictions are compared to published studies and references are made to their use in management and policy development.

Conclusions The development and utility of web platform software based on the PBDM paradigm is outlined, which aims to guide non-experts in formulating realistic models and gathering the biological data to parameterize them while providing links to relevant weather data for running the models and tools for GIS mapping and statistical analysis of model output for policy and management development. Numerous published heritage PBDMs that the web platform software would make available are summarized in the Supplementary Information.

*Correspondence:
Andrew Paul Gutierrez
CASAS.Global@berkeley.edu
Full list of author information is available at the end of the article

Keywords PBDM Web platform, Invasive species, Population ecology, Physiologically based demographic models, Time-varying life tables, GIS, Tri-trophic

Introduction

How to analyze agro-ecological and eco-epidemiological important species problems holistically to inform management and policy development in both developed and developing economies under ongoing climate change over wide geographic landscapes remains an open question and has economic consequences. The effectiveness of management expenditures for invasive and native pest species is difficult to assess due to a lack of appropriate models and standardized measurements across taxonomic, spatial, and temporal scales. Since 1960, worldwide management expenditures for invasive species have totaled at least US$95.3 billion (2017 values), which is 12 times less than damage costs (US$1,130.6 billion) [1]. Pimentel et al. [2] opined that invasive species cause more than US$140 billion in losses annually in the United States, while annual losses in the European Union are US$28 billion with projected losses of US$148 billion by 2040 [3]. Loss in subsistence staple food crops (e.g., cassava, maize, millet, sorghum) and in veterinary and human health in Africa from pest species are large but not well documented [4, 5] and beg serious attention.

Commonly, researchers study the biology of native and invasive species without a unifying framework resulting in myriad studies of limited generality. Readily available species distribution models (SDMs) correlate rough measures of weather and other variables to records of species presence and are the mainstay for prospectively predicting the geographic distribution and relative favorability for invasive species [6]. While SDMs provide important information, they have limited capacity to examine the weather-driven dynamics and interactions of species required to inform management and policy development. We propose that weather-driven physiologically based demographic models (PBDMs) circumvent many of these limitations and augment SDMs and other research approaches. Specifically, PBDMs capture the weather-driven time-varying dynamics of species in agricultural and natural systems independent of time and place constraints required to develop strategic and tactical responses to manage plant–herbivore–natural enemy interactions and vectored medical and veterinary disease problems under extant and climate change weather across vast geographic landscapes [7, 8].

In this study, we show how the same relatively simple model structure is used to model the biology and analyze the dynamics, and prospective geographic distribution and abundance of thirteen invasive species with disparate biology across Africa and other regions as appropriate. The 13 invasive species systems examined (with a total of 20 species modeled) are:

(1) New world screwworm fly (*Cochliomyia hominivorax* (Coquerel));
(2) Olive (*Olea europaea* L.) and olive fly (*Bactrocera oleae* (Rossi));
(3) Asian brown marmorated stinkbug (*Halyomorpha halys* (Stål)) and three of its parasitoids;
(4) South American tomato pinworm (*Tuta absoluta* Meyrick);
(5) African false codling moth (*Thaumatotibia leucotreta* (Meyrick));
(6) Fall armyworm (*Spodoptera frugiperda* (J. E. Smith));
(7) Citrus (*Citrus* spp.), Asian citrus psyllid (*Diaphorina citri* Kuwayama), its parasitoid (*Tamarixia radiata* (Waterston)), and the bacterial pathogen ('*Candidatus* Liberibacter asiaticus');
(8) Asian tiger mosquito (*Aedes albopictus* (Skuse));
(9) Yellow fever mosquito (*Aedes aegypti* (L.));
(10) Mediterranean fruit fly (*Ceratitis capitata* (Wiedemann));
(11) Melon fly (*Bactrocera cucurbitae* (Coquillett));
(12) Oriental fruit fly (*Bactrocera dorsalis* (Hendel)); and
(13) Mexican fruit fly (*Anastrepha ludens* (Loew)).

A second related *raison d'etre* is to argue for the development of a modeling platform (see Supplemental Materials appendix, Fig. 1) to enable researchers and policy makers to develop and run PBDMs via the Web to analyze pest problems for management and policy development. The Web platform would guide researchers in assembling the relevant data on the weather-driven biology of species and species interactions required to parameterize PBDMs, provide linkages to weather files to run the models for varying time periods in a georeferenced lattice across vast regions (e.g., Africa), software to summarize the multi-year runs in any lattice cell, and seamless linkages to GIS and statistical software to map and analyze the results (steps, Fig. 1A–D). The PBDM Web platform would enable modeling biological complexity as depicted in Fig. 1E [8, 9]. Currently, steps A through D in Fig. 1 are implemented as separate processes that the Web platform

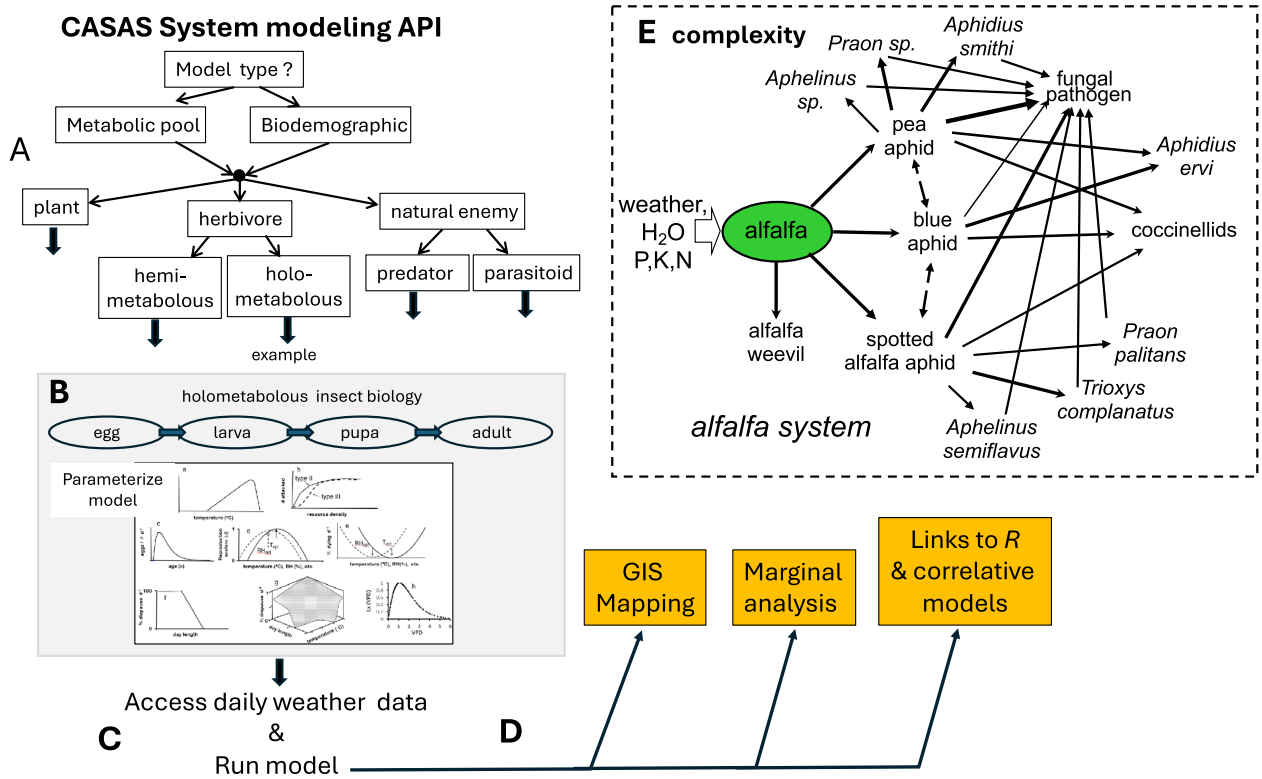

Fig. 1 Proposed PBDM Web platform for developing and implementing physiologically based demographic models (PBDMs): **A** decision path for system model development; **B** sub model parameterization (see Figs. 2, 3 and 4); **C** access weather files and run models; **D** create output files for mapping and analysis; and **E** an example of the complexity modeled with PBDMs (e.g., [9, 13]). Note in Fig. 1A, hemi- and holometabolous life cycles may occur in any arthropod trophic level

would seamlessly integrate. In this study, statistical and climate change analyses are not conducted, but relevant examples are reviewed in the discussion. The feasibility of the PBDM Web platform has been assessed successfully based on seed funding provided by the McKnight Foundation under the Global Collaboration for Resilient Food Systems (see https://www.ccrp.org/grants/python-based-platform-to-evaluate-crop-pest-systems/).

In addition, the PBDM Web platform would have links to the executables of heritage models written in various computer languages (e.g., Fortran, Pascal, C++, Python; see Supplemental Materials Table 1). A prototype Web Application Programming Interface (API) was initially developed and implemented by the EU-funded MED–GOLD project (https://doi.org/https://doi.org/10.3030/776467) as a component of its Information and Communication Technology (ICT) platform, and further developed and released as open source software (https://github.com/casasglobal-org/pbdm-workflow) with support of project TEBAKA (https://www.dtascarl.org/en/projects-and-initiatives/use-case-technology-transfer/tebaka/) and the McKnight Foundation. Using the PBDM Web API, the heritage Pascal-based olive/olive fly model [10] was implemented and used to analyze olive production in Andalusia, Spain with the results mapped using the open-source GRASS GIS [11]. The full suite of geospatial software based on GRASS GIS together with the associated GIS data sets [12] that have been used in published PBDM analyses (see https://www.casasglobal.org/publications/) was released as open source (https://github.com/casasglobal-org/casas-gis) and is being updated and unified into a Python app.

Model overview

PBDMs fall under the ambit of time-varying life tables (TVLTs; cf. [14]), the theoretical bases of which were reviewed by Gutierrez [7, 15], Gutierrez et al. [16], and Mills and Gutierrez [17]. The initial impetus for the development of PBDMs/TVLTs was the early work of R.D. Hughes in Australia [18], N.E. Gilbert in Canada [19], and Gutierrez and Baumgärtner in California [9]. The development of PBDMs flourished under the auspices of the NSF/EPA/USDA funded Huffaker Projects during the 1970s (https://nap.nationalacademies.org/read/9649/chapter/9) enabling deconstruction and analyses of some agricultural systems sufficient to

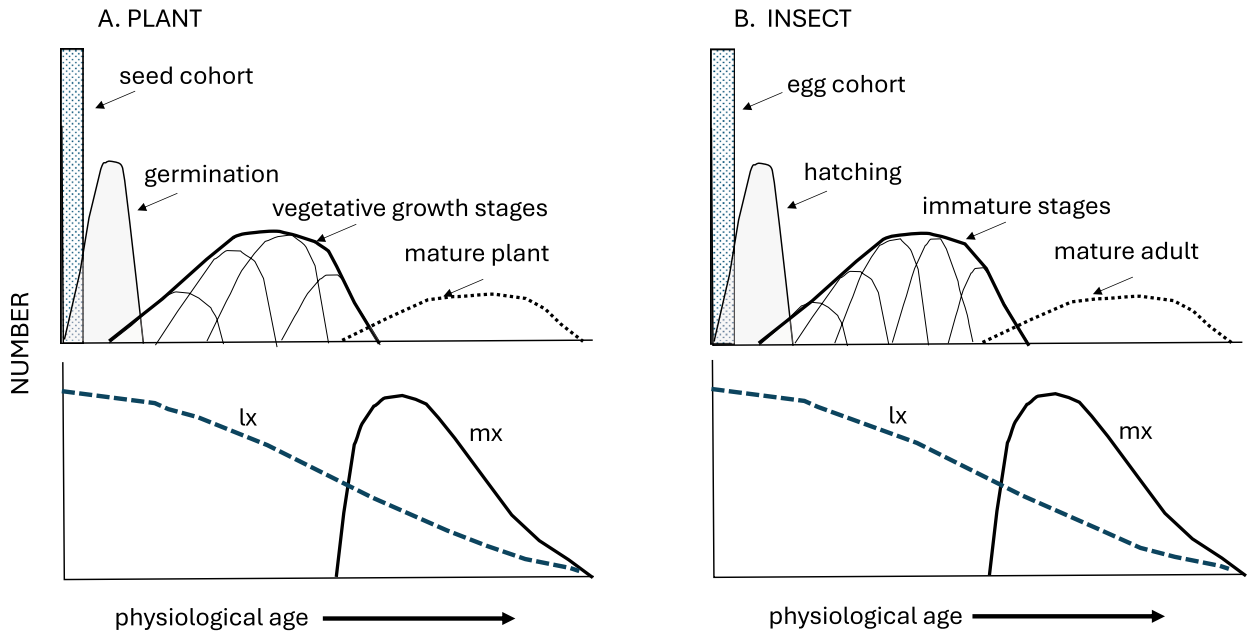

Fig. 2 Analogous developmental stages of a plant and an insect with the bottom panel characterizing survivorship (*lx*) and reproductive profiles (*mx*). Note that the developmental times of individuals initiated at the same time have distributed developmental rates

provide sound management recommendations. Two recent holistic PBDM/TVLT analyses of complex systems are the coffee system [20] and the hybrid Bt cotton system in India [21, 22]. If sufficiently complete, the models can be used as the objective function in economic analyses of agroecological problems [21, 23, 24]. PBDMs can be updated as new data becomes available without changing the basic structure of the model.

Multitude life history strategies occur in nature, but the developmental biology of all multicellular organisms have analogous processes allowing the same modeling paradigm to be used [7, 25]. For example, plants may germinate from seed, grow vegetatively, and mature and produce seed (Fig. 2a), while an animal may start as an egg, hatch, and develop as an immature organism passing through various life stages to become a reproducing adult (Fig. 2b). Stylized age-specific survivorship (*lx*) and reproductive (*mx*) profiles for plants and arthropods are illustrated in the respective lower panels of Fig. 2. The life span of the organisms may be hundreds of years (e.g., redwoods) or a few days (e.g., water fleas), but the underlying patterns are the same. Furthermore, the developmental biology of a species may be determinate or indeterminate, and the developmental times of a cohort initiated at the same time have mean and variance.

To capture the field biology of species, age-structured PBDM/TVLT (hereafter PBDMs) have been developed using two approaches (Supplementary Materials Table 1): (1) the metabolic pool (MP) approach of energy acquisition and allocation, and (2) the biodemographic function (BDF) approach [7]. In developing tritrophic system models, all the models may be MP- or BDF-based, or they may be a mix of the two approaches (e.g., Fig. 3b, c). As shown below, the two approaches are related.

Metabolic pool approach (MP)

MP models are bioeconomic models of how organisms acquire and allocate resources and have been used to model the growth and development of plants and arthropods [26], and for harvesting by human firms [23]. Physiological studies by de Wit and Goudriaan [27] and colleagues in the Netherlands on plant growth and development provided early impetus globally for the development of MP plant models. The models sought to capture weather-driven processes of resource acquisition and allocation (i.e., photosynthate) for plant growth and development, by analogy first to egestion, then to respiration, conversion costs and to growth and reserves if immature, and to reproduction by mature organisms. Gutierrez et al. ([26, 28], see [29]) used these notions to develop demographic models of a plant canopy composed of age-mass structured populations of leaves, stem, root, and an age-mass-numbers structured population of fruit (Fig. 3b). In MP-based PBDMs, the ratio of the amount of resource obtained (*S*, supply) and the physiological demand for resources (*D*, demand) regulates

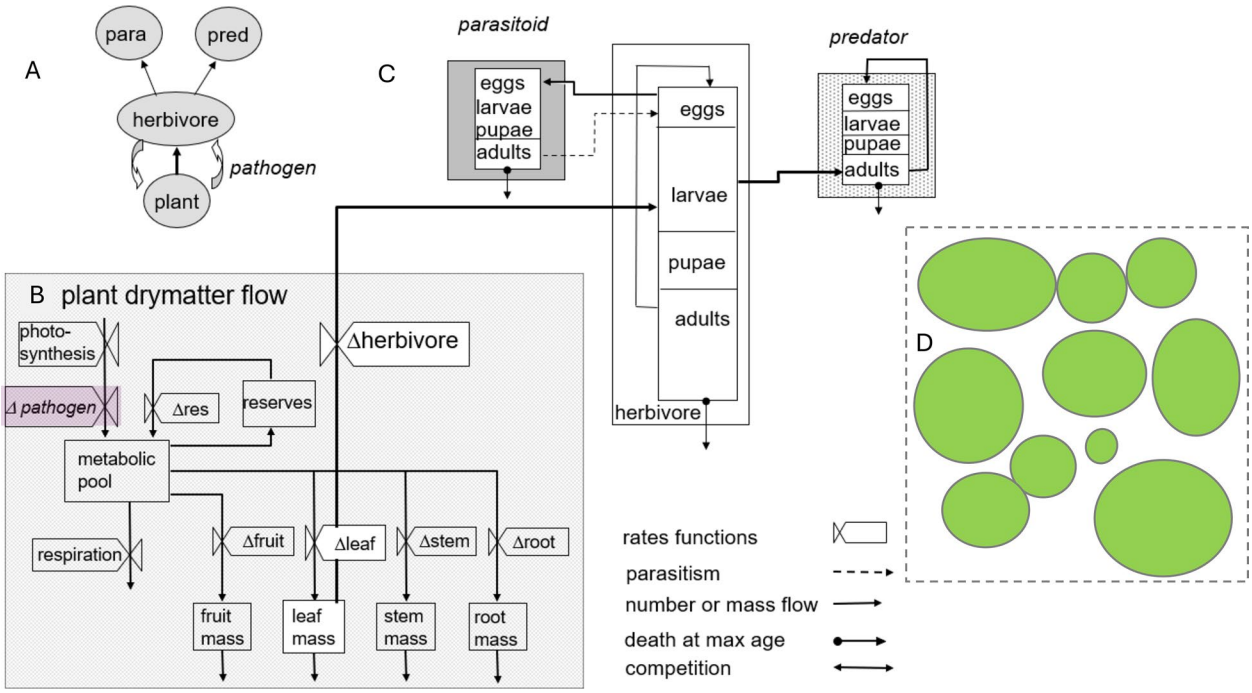

Fig. 3 PBDM tri-trophic system: **A** energy/dry matter flow in a tri-trophic system, **B** energy flow within a plant as affected by a pathogen, **C** to higher trophic levels with the herbivore attacking leaves [7], and **D** a population of plant each with herbivore/natural enemy populations on them with movement between plants [30]

all vital growth and developmental rates. In plants, *D* for photosynthate is the sum of the genetic maximum growth rates of all plant subunits under conditions at time *t* corrected for metabolic costs (e.g., egestion, respiration, and conversion costs). The supply of photosynthate is always less than the demand due to imperfect search for resources (e.g., light, water, and nutrients) with the ratio $0 < S/D < 1$ estimating the success rate that determines the realized growth, death, and reproductive rates [15, 16] (see below). Similar models for populations of herbivores and natural enemies (parasites, predators, and pathogens, see below) inhabiting the canopy have been developed. Herbivores attack specific plant organs in an age-specific manner, and natural enemies attack herbivores in an age-specific manner (e.g., Fig. 3C). The dynamics of the system are moderated by plant bottom-up and herbivore/natural enemy top-down effects on species-specific *S/D* ratios (Fig. 3B, C).

The canopy model was expanded to a population of individual plants of different sizes, ages, and areas for growth that compete with neighbors for light, water, and inorganic nutrients (inset Fig. 3D) [30]. Furthermore, each plant has interacting populations of herbivores and natural enemies (parasites, predators, and pathogens) on them, with species *S/D* ratios influencing movement rates of mobile stages between plants.

Biodemographic function approach (BDF)

Data to develop MP-based PBDMs are often unavailable, and the simpler PBDM/BDF approach is an alternative. Specifically, species birth and death rates can be estimated from age-specific life table studies conducted under different temperatures and other conditions (e.g. [31]), the vital rates of which are the outcomes over the life cycle of a cohort of organisms of how the members acquired and allocated resources, developed, survived, and reproduced. These rates are the result of metabolic pool processes under the experimental conditions and can be used to parameterize the BDFs presented in a stylized way in Fig. 4. In practice, the BDFs are invariably not symmetrical, and experiments to characterize critical mortality rates at extreme conditions must be estimated in separate experiments.

Developmental rates—The developmental rates of poikilotherm plants and animals and their sub-stages (*r(T)*, Fig. 4A) are largely functions of temperature [32], but other factors such as nutrition can affect development rates. A simple model (Eq. 1) with parameters a and b captures the effects of temperature on *r(T)*, where *d(T)* is development time in days at temperature *T* with lower (θ_L) and upper (θ_U) thermal thresholds for development (see Fig. 4A) with θ_I being the inflection point, where *r(T)* departs strongly from linearity and declines to zero. A similar function is by Briére et al. [33]:

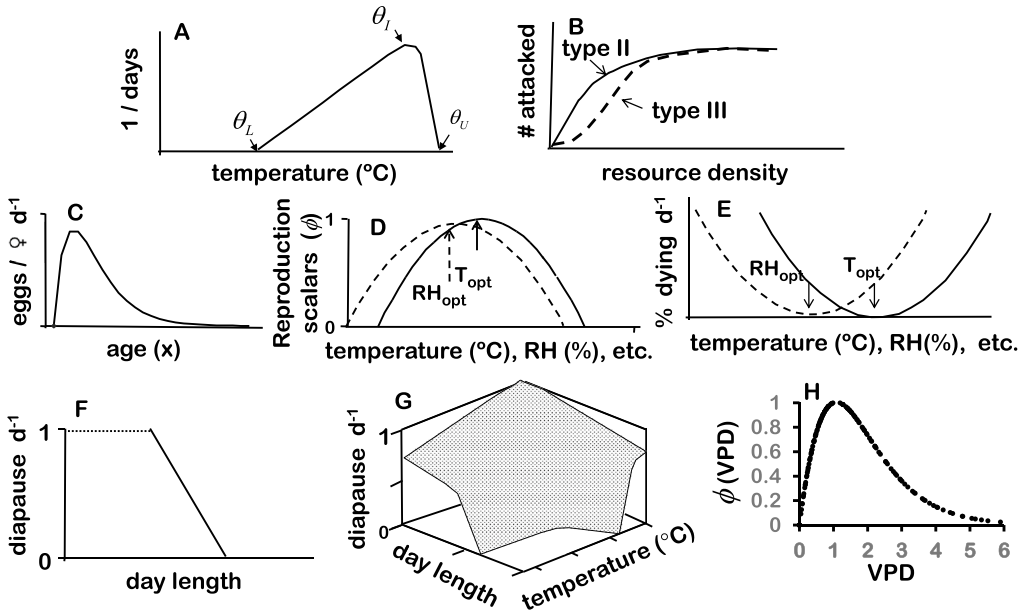

Fig. 4 Stylized biodemographic functions (modified from [8]): **A** rate of development on temperature, **B** resource acquisition (i.e., the functional response), **C** age-specific reproductive profile at the optimum temperature, **D** temperature and relative humidity scalars to correct reproduction from the optimum, (**E**) mortality rate per day at different temperatures and relative humidity, **F**, **G** the proportion entering dormancy due to photoperiod and due to photoperiod and temperature, respectively, and **H** a scalar function for oviposition due to vapor pressure deficit

$$r(T) = 1/d(T) = \frac{a(T-\theta_L)}{(1+b^{T-\theta_I})} \tag{1}$$

The physiological developmental time constant (${}^s\Delta$) for each species or life stage in degree days (*dd*) is estimated in the linear range of favorable temperatures as ${}^s\Delta = d(T) \times (T - {}^s\theta_L)$. The daily increment of physiological time at time t and temperature T is ${}^s\Delta x(T(t)) = {}^s r(T(t)){}^s\Delta$. Hence, on average a cohort of individuals initiated at time t_0 completes development when $\int_{t_0}^{t} {}^s r(T(t))dt = 1$ in continuous form, or $\sum_{t_0}^{t} {}^s\Delta x(T(t)) = {}^s\Delta$ in *dd* units for age x in our discrete time models. In multi-species systems, species (and their stages) may develop on different aging scales.

Functional response—All organisms are consumers and acquire resources through search (i.e., the functional response, Fig. 4B) that may be influenced by several factors. Critical innovations for PBDM development were the demand-driven parasitoid ratio-dependent Gilbert–Fraser functional model ([34]; Eq. 2i), and the derived Gutierrez–Baumgärtner predator form ([7]; Eq. 2ii). The parasitoid form is appropriate when a host can be attacked more than once by one or more consumers (e.g., fruit or parasitoid host). In contrast, the predator form posits the resource is consumed and unavailable to other consumers, be it a leaf capturing a quantum of light or a coccinellid beetle consuming an aphid:

$$S = R\left(1 - e^{\frac{-DN}{R}(1-e^{\frac{-\alpha R}{DN}})}\right) \tag{2i}$$

$$S = ND\left(1 - e^{\frac{-aR}{DN}}\right) \tag{2ii}$$

In both functional response models, R is the resource level (be it energy, mass, or numbers), D is the per capita demand, α is the proportion of the available resource that can be found during a time step, and S is the amount of the resource acquired by the consumer population N. Note that if α is a constant, the model is type II (solid line in Fig. 4B), but is type III (dashed line in Fig. 4B) if α is a function of consumer density. The ratio $0 < S/DN < 1$ is a metric of resource acquisition success by the population and is used to scale vital rates from the maximum.

The demand component of the functional response model can accommodate age structure. For example, if adult female parasitoids seek hosts (Eq. 2i), the total oviposition site demand by all females in the population ($\hat{D}(t)$) at time t is the sum of the product of the age-specific per capita fecundity per day ($f(i, T_{opt}) = ci/(1+d^i)$; Fig. 4C) at the optimal temperature (T_{opt}) and the number of adults (${}^A N(i,t)$) of age i corrected for the sex ratio (*sr(t)*) that may change over time (Eq. 3i):

$$\hat{D}(t) = sr(t) \sum_{i=1}^{k} f(i, T_{opt})^{A} N(i,t) \tag{3i}$$

$$\hat{D}(t) = sr(t) \prod_{j=1}^{J} \phi_j(\cdot, t) \sum_{i=1}^{k} f(i, T_{opt})^{A} N(i,t) \tag{3ii}$$

Oviposition demand may be limited by J factors, say temperature ($0 < \phi_T(t) \leq 1$) with lower and upper oviposition thresholds, relative humidity ($0 < \phi_{RH}(t) \leq 1$) (Fig. 4D), or host age preferences, nutritional effects, and behavior, etc. These limiting factors may be viewed as concave probability functions, and are included in Eq. 3ii as $0 \leq \prod_{j=1}^{J} \phi_j(\cdot, t) \leq 1$ [7]. The total population demand $\hat{D}(t)$ replaces DN in eqns. 2i, ii. Similarly, the age-structured demand of a predator drives its search for resources, be it plant leaves searching for light, roots searching for water and nutrients (e.g., *N, P, K*) or an insect predator searching for prey—all are the same functional processes (Eq. 2ii).

Detailed physiology or behavior can be added to model Eq. 3ii without complication. For example, a demand-driven version of the mechanistic Ritchie et al. [35] water balance model has been used to estimate water *S/D* effects (i.e., $0 < \phi_W(t) \leq 1$) on photosynthesis and ground water balance computations. Desiccation may also affect organism development, survival, and reproduction, and may be estimated as a function of vapor pressure deficit (e.g., $0 < \phi_{VPD}(t, T, RH) < 1$) [36] that is a measure of the atmospheric desiccation strength in kPa (kilopascals) [37].

Mortality rates—The shapes of the BDF for mortality on temperature and relative humidity illustrated in Fig. 4E are symmetrical, but the shapes may vary greatly as species may have very different tolerance to temperature extremes and to other factors. Average mortality rates in the favorable range can be estimated as the average slope of the *lx* functions at each temperature in the life table studies (see Fig. 1). However, species may experience extreme temperatures, relative humidity or other factors in the field that are not amenable to life table analyses, hence mortality rates must be estimated by exposing cohorts of organisms to these conditions. Furthermore, corrections can be made to accommodate daily fluctuating temperature extremes and conditions in protected refuges. The mortality rate (${}^{s}\mu$) is implemented as the product of say the L survivorship rates (i.e., $0 \leq {}^{s}\mu = 1 - \prod_{l=1}^{L} (1 - {}^{s}\mu_l(\cdot, t)) \leq 1$), and is an application of von Liebig's Law of the Minimum [38].

Dormancy—Species may evolve dormancy mechanisms to escape unfavorable periods that may be triggered by temperature, moisture deficits, daylength and other factors. Figure 4F shows a simple relationship of dormancy to day length, and Fig. 4G shows a more complex relationship on temperature and photoperiod (see [39]). Capturing entry to and exit from dormancy may determine how well the model captures the biology determining the geographic distribution and relative abundance and dynamics of a species. Entry to and exit from diapause may be viewed as a dynamic stage-structured process [40].

Population dynamics models

Cohort members entering the population at the same time may have different developmental times, and population dynamics models must accommodate this. Relevant models were reviewed by Gutierrez [7], Di Cola et al. [41], and Buffoni and Pasquali [42]. For simplicity and ease of implementation, the discrete form of the time-invariant and time-varying Erlang distributed-maturation time demographic models are used here for all of the species and their life stages (see [43–45]) and were parameterized using MP and/or BDF biology. The dynamics of a life stage s with $k = 1, 2, \ldots, {}^{s}k$ age classes can be viewed as composed of ${}^{s}k$ dynamics equations (Eq. 4; [7, 44, 46]). The forcing variable is temperature (T), with time (t) being a day (d) that from the perspective of poikilotherm species is of variable length in physiological time units (i.e., $0 \leq {}^{s}\Delta_x(T(t))$ in degree days (dd)), or proportional development (${}^{s}r(T(t))$). Species (and life stages) may have different mean developmental times (${}^{s}\Delta$) and temperature thresholds allowing their development to proceed on different time scales (see Fig. 4A). The biological data to parameterize PBDMs are often means collected at daily or longer time intervals, but shorter time steps may be important when daily fluctuation to temperature extremes adversely affect death and other vital rates. Following the notation of Di Cola et al. ([41], page 523), the dynamics of the i^{th} age class of stage s is as follows:

$$\frac{d^{s}N_i}{dt} = \frac{{}^{s}k \cdot {}^{s}\Delta_x}{{}^{s}\Delta} \left[{}^{s}N_{i-1}(t) - {}^{s}N_i(t) \right] - {}^{s}\mu_i(t) {}^{s}N_i(t). \tag{4i}$$

In terms of flux, ${}^{s}n_i(t) = {}^{s}N_i(t) {}^{s}v_i(t)$, where ${}^{s}v_i(t) = \frac{{}^{s}k}{{}^{s}\Delta} \Delta_x(t)$, and

$$\frac{d}{dt} \left[\frac{{}^{s}\Delta {}^{s}n_i(t)}{{}^{s}k} \right] = {}^{s}n_{i-1}(t) - {}^{s}n_i(t) - {}^{s}\mu_i(t) {}^{s}n_i(t) \frac{{}^{s}\Delta}{{}^{s}k}. \tag{4ii}$$

The state variable ${}^{s}N_i(t)$ is the density of the i^{th} age class (mass or numbers), the total density in life stage s

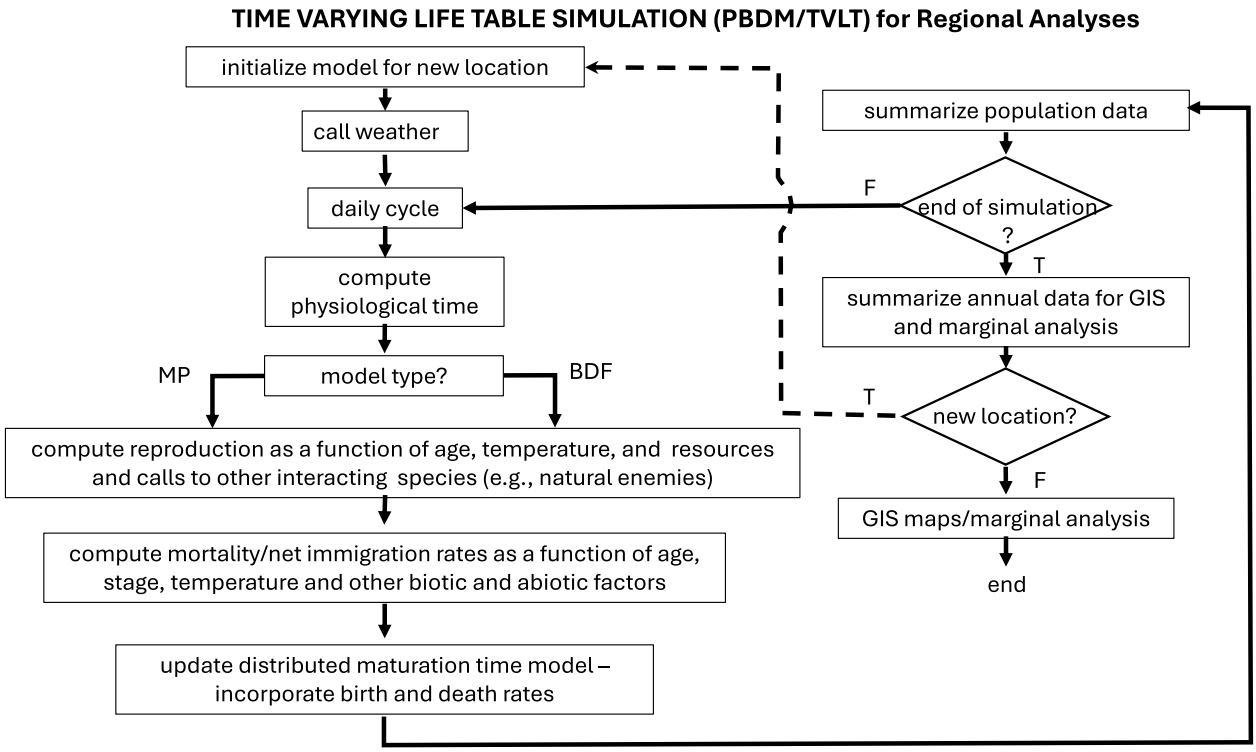

Fig. 5 Daily flow diagram of a physiologically based demographic model using metabolic pool (MP) or biodemographic functions (BDFs) approaches. The dashed arrow shows the transition between locations

is ${}^{s}N(t) = \sum_{i=1}^{k} {}^{s}N_i(t)$, and ${}^{s}\mu_i(t)$ is the proportional age-specific net loss rate due to temperature, net immigration, growth in mass dynamics models, and other L factors (see above) during ${}^{s}\Delta_x(T(t))$. Ignoring stage notation, new individuals enter the first age class of a stage ($i=1$), flows occur via aging between age classes and between stages at temperature dependent rates, with surviving adults exiting as deaths at maximum age of the species ($i={}^{s}k$). Absent mortality, the theoretical distribution of cohort developmental times of stage s may be estimated by Erlang parameter ${}^{s}k = {}^{s}\Delta^2/{}^{s}\sigma^2$, where σ^2 is the variance of average developmental time ${}^{s}\Delta$. In practice, ${}^{s}k$ is an approximation from data. Furthermore, developmental times (rates) may vary with nutrition and other factors [7], and given appropriate data can be easily accommodated using the time-varying form of the model ([45] see [47]). Last, because of non-linearities and time-varying nature, the model can only be evaluated numerically [48]. The numerical solution for Eq. 4ii can be found in Abkin and Wolf [43], and as implemented here in Gutierrez ([7] pages 157–159).

The algorithm (Fig. 5) shows the computation cycle of the daily birth–death rates and aging for a species (Eq. 4) at a specific location or all georeferenced lattice cells (the dashed line) across the vast geographic landscape of Africa. The life history variables for all life stages of all species are updated daily in each lattice cell in runs of several years, and the detailed age-stage dynamics of system components in any lattice cell may be graphed (e.g., [49]). The flow diagram also shows points of linkages to trophic interactions. The run time for the daily computations over 10 years at any location is ~ 5–10 s. The output interval (daily, monthly, or yearly) may be specified, and selected georeferenced output variables are written to year-specific text files. Ignoring first-year results when the model is assumed equilibrating to site-specific conditions, averages of annual variables across years ($\bar{x}$), standard deviation (std) and coefficient of variation (CV) are computed for each lattice cell. Selected summary variables are mapped using GIS, and marginal analysis ($\partial y/\partial x_i$) may be performed on the full data set to estimate the impact on some dependent variable y of independent variable x_i (i.e., step D in Fig. 1, [7]). Movement of organisms between lattice cells is not included in the model.

Weather data

The growth and abundance of a species at a geographic location emerges in response to local resource availability, interaction with other species, and weather. From the perspective of an ectotherm species, climate change is simply another weather pattern, and in the extreme

determines whether a species can persist and/or invade new areas. The effects of climate change on the systems are not included in this study due to space constraints, but numerous examples are found in the cited references (e.g., see Supplemental Materials Table 1). Daily weather for 40,691 georeferenced 25 × 25 km lattice cells across Africa were sourced from the global Climate Forcing Data Set for Agricultural Modeling AgMERRA [50] created as an element of the Agricultural Model Intercomparison and Improvement Project (AgMIP, https://agmip.org/). AgMERRA consists of daily time series of weather data over the 1980–2010 period and can be accessed through the Goddard Institute for Space Studies (GISS) of the National Aeronautics and Space Administration (NASA, https://data.giss.nasa.gov/impacts/agmipcf/). However, because of computation constraints on a laptop computer, only 10,164 of the lattice cells (alternating rows and columns of the lattice mesh) were used to capture the relevant details of each study. A maximum of six weather variables are used to run the PBDMs (maximum and minimum temperature, precipitation, solar radiation, relative humidity, and wind). Climate model data can be used to run the models for studies on climate change's effects on species, but this is beyond the scope of this study (see Supplemental Materials, for examples).

GIS mapping

The open source GIS software GRASS [51, 52] (see http://grass.osgeo.org/) was used to map PBDM output data. All GIS data layers used in the analysis are available open access [12], and most were sourced from the public domain repository *Natural Earth* (https://www.naturalearthdata.com/). Inverse distance weighting or bicubic spline interpolation is used in mapping model output as a continuous raster surface. The smoothed spatial patterns reflect the site-specific effects of weather on the biology of the species, and the resolution of the lattice grid. Note that irrigated areas may provide microhabitats in otherwise unsuitable arid areas, but this is not included in the study.

Results

The goals of the study are twofold: (1) to demonstrate the ease of development and the utility of PBDMs and (2) to advance the need for the development of a Web platform (Fig. 1) to enable PBDM development by non-experts. The Web platform would enable research and policy groups globally to implement PBDM/GIS analyses like those presented here and extend the analysis for management and policy development (see Discussion). Some of the PBDMs reported herein are new and others published. Varying levels of biological data were available to parameterize the PBDMs in this study with the full extent of the available data found in the cited references. We note that all the models can be extended and improved with additional components and data, as PBDMs function as dynamic modular libraries of developing knowledge about biological systems that can be incorporated as it becomes available.

Rainfall—The time and quantity of rainfall is a major factor limiting the geographic distribution and abundance of agricultural and native species, and as background the average annual precipitation (masked > 2500 mm) during 2001–2010 and the associated coefficients of variation as a percent (CV) across Africa are mapped in Fig. 6A, B, respectively. Rainfall varies widely from areas of high rainfall in West-Central Africa to low rainfall in the deserts in the Sahara and the southern reaches of Africa. Highest CVs occur in the Saharan areas of northern Africa. The major rivers of Africa are indicated as white lines in GIS, Fig. 6A.

Analysis of species distribution and relative abundance

(1) New-world screwworm

The new world screwworm (*Cochliomyia hominivorax* (Coquerel) (Diptera: Calliphoridae)) is indigenous to subtropical–tropical areas of South, Central and North America and the Caribbean. The fly causes myiasis in warm-blooded animals including humans and hence its egg and larval stages develop at hosts body temperatures (~ 38 °C for cattle). The fly lacks a dormant stage, and the life stages have high lower and upper thermal thresholds for development (i.e., 14.5 °C and 43.5 °C, respectively; Fig. 7A), and the optimum temperature for egg production is ~29 °C within a range of 14.5–43.5 °C [53, 54]. Adults are sensitive to moderately cold and high temperatures (Fig. 7B, C) with lowest mortality occurring at ~ 27 °C.

In North America, the prospective northern limit of permanence for screwworm is the southern tip of Texas and south Florida as characterized by the annual sum of daily mortality rates > 5 for adults and pupae below and above the optimum of 27.2 °C (Eq. 5i, ii; [54]):

$$ {}^{low\ T}\hat{\mu}_{year} = \sum_{t=1}^{365} \mu(T(t) \le 27^{\circ}C) \tag{5i} $$

$$ {}^{high\ T}\hat{\mu}_{year} = \sum_{t=1}^{365} \mu(T(t) > 27^{\circ}C) \tag{5ii} $$

Historically, periodic outbreaks of myiasis occurred in wildlife and livestock during summer in the southwestern

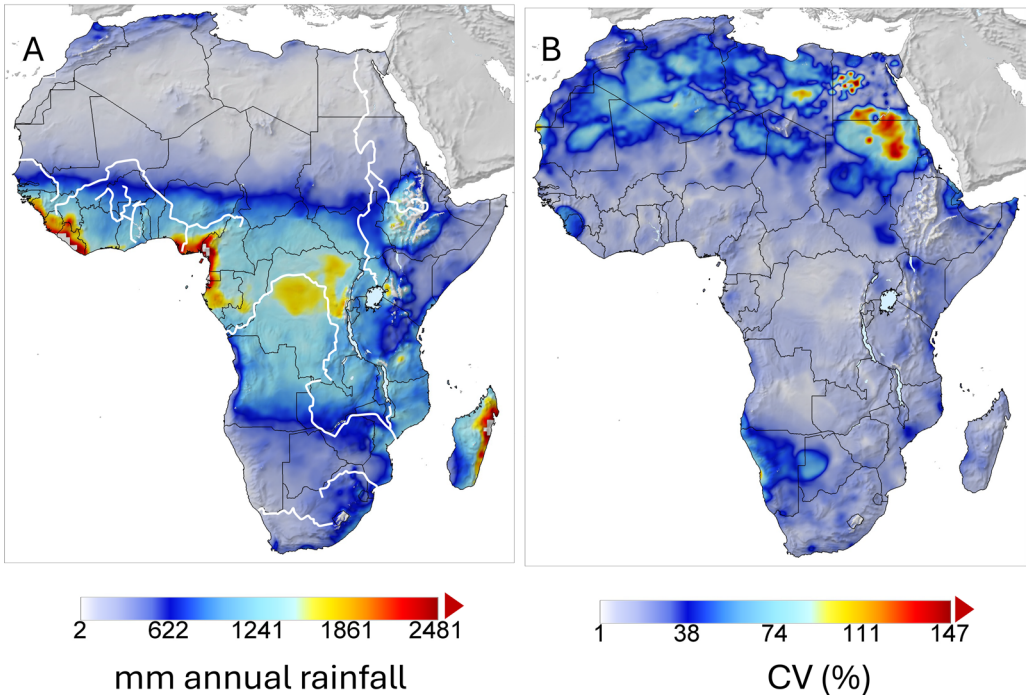

Fig. 6 Map of average annual rainfall for the period 2001–2010 masked at 2500 mm with the major rivers indicated as white lines (**A**), and (**B**) coefficients of variation as a percent masked at 150%

USA (principally Texas) when adult migrants invaded on North American monsoon winds from areas of permanence in northern Mexico (see [54]). In the late 1960s, the USDA implemented a sterile insect technique (SIT) eradication program in the southern USA that was later extended to the Darian Gap in Panama. Screwworm proved to be an ideal candidate for SIT eradication using sterile males, because males are polygynous but a female mates only once, field populations are low, and although the fly has a high reproductive potential, endemic field population growth is limited by the availability of wound sites for oviposition. Despite an estimated ~ 1.25% efficacy rate of released SIT males, eradication in endemic areas of tropical Mexico and Central America is attributable to SIT as the added mating competition on the reproductive success of wild male populations leads to native mate-limited extinction [54].

Screwworm was accidentally introduced to the area of Tripoli, Libya during 1988, and SIT eradication was begun in December 1990 (effectively 1991) [55]. However, PBDM analysis suggests that the area around Tripoli is unfavorable for fly permanence, with the vast desert area to the south being unfavorable for the fly due to high temperatures, aridity, and lack of water resources for vertebrate hosts (Fig. 7D, [53]). El-Azazy [56] posited that establishment of screwworm along the Nile River (white line) could provide a gateway southward through arid regions of Egypt and Sudan leading to invasion of highly favorable tropical sub-Saharan Africa.

Using ${}^{low\ T}\hat{\mu}_{year} = 5$ (Eq. 5i) as a threshold, the favorable areas in Africa are sub-Saharan tropical Africa with decreasing favorability northward and southward due to increasingly cold weather (Fig. 7E). Areas of the Sahara are also unfavorable due to high summer temperatures (${}^{high\ T}\hat{\mu}_{year} > 5$; Fig. 7F).

As a final note, the biological data available to develop the PBDM for screwworm were sparse despite approximately one billion US$ spent on screwworm SIT eradication efforts in North and Central America. A comprehensive biology of screwworm remains to be published. The SIT screwworm incidence data for Texas are available on request.

(2) Olive/olive fly

Olive (*Olea europaea* L.) is an ancient, drought-tolerant long-lived ubiquitous crop in the Mediterranean Basin that originated in Asia Minor 6000–8000 years ago [57]. The geographic distribution of olive is limited northward by freezing temperatures and southward by high temperature, and absent irrigation, by low rainfall [58–60]. The oligophagous olive fly (*Bactrocera oleae* (Rossi) (Diptera: Tephritidae)) is a major pest of olive, and both species were modeled by Gutierrez et al. [10]

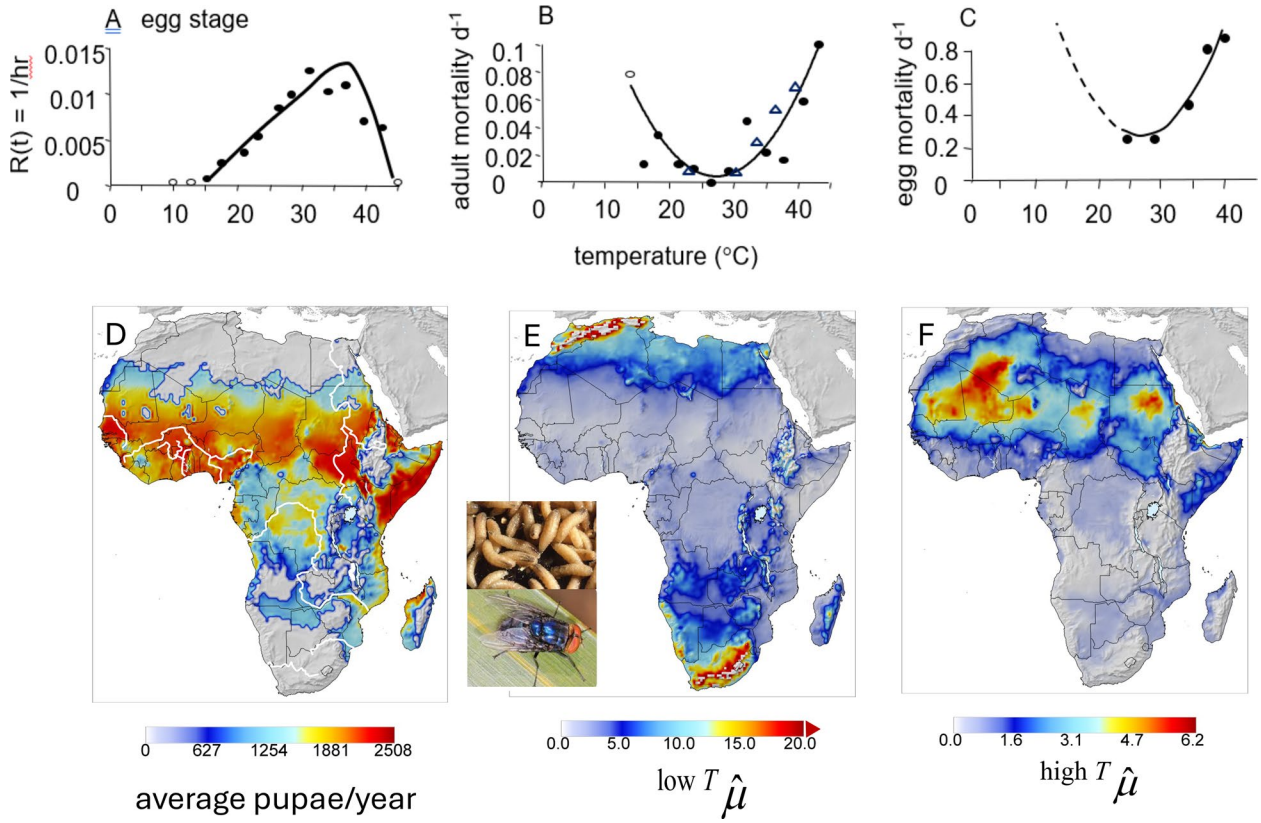

Fig. 7 New world screwworm: biodemographic functions (**A**) egg developmental rate, (**B**) adult mortality/day on temperature, **C** and egg mortality rate on temperature, and maps of (**D**) prospective geographic distribution and average relative abundance (i.e., favorability) of screwworm pupae, **E** mean cumulative annual cold weather mortality rate (${}^{low\ T}\hat{\mu}_{year}$) masked at 20, and **F** average cumulative annual hot weather mortality rate (${}^{high\ T}\hat{\mu}_{year}$) (see text). The major rivers of Africa are illustrated as white lines in (**D**)

and Ponti et al. [61]. An important factor is the wider thermal limits in olive relative to olive fly (Fig. 8A–C).

Relative olive yield and cumulative annual olive fly pupae are used as metrics of favorability. For comparative purposes, the simulated prospective geographic distribution and relative abundance of olive fly in the Mediterranean Basin is mapped in Fig. 8D. Using the same initial conditions, olive yield and olive fly densities in Africa in non-irrigated areas are mapped in Fig. 8E, F in areas above 500 mm annual rainfall (the lower limit for commercial yields under rain fed conditions, [62]). The results show that cooler regions of East Africa and southward into South Africa are favorable for olive, with favorability in areas of Saharan Africa and near coastal areas of North Africa with sufficient rainfall (and irrigation). Olive fly abundance mirrors the distribution of olive, but because the fly is less tolerant of high temperatures, only moderate fly populations are predicted in favorable areas of Africa compared to the Mediterranean Basin (Fig. 8D vs. F).

(3) Brown marmorated stink bug

The highly destructive polyphagous Asian brown marmorated stinkbug (BMSB), *Halyomorpha halys* (Stål) (Heteroptera: Pentatomidae) invaded North and South America, Europe, and Caucasus region, and here we examine its potential to invade Africa. A tri-trophic PBDM system model of the interactions of BMSB and its parasitoids as forced by weather was used to evaluate prospectively the geographic range of the pest and the impact of natural enemies on its biological control under extant and climate change weather in the Palearctic region [63]. The same model and initial conditions were used to evaluate the potential of BMSB to invade Africa.

BMSB is a temperate species with lower and upper thermal thresholds of 12.1 °C and 35 °C, respectively, and an optimal temperature for oviposition of ~ 26 °C. The pest is moderately cold tolerant and overwinters as an adult. The analysis includes the effects of two hymenopterous stenophagous egg parasitoids (*Trissolcus japonicus* (Ashmead) and *T. mitsukurii* (Ashmead)), the egg

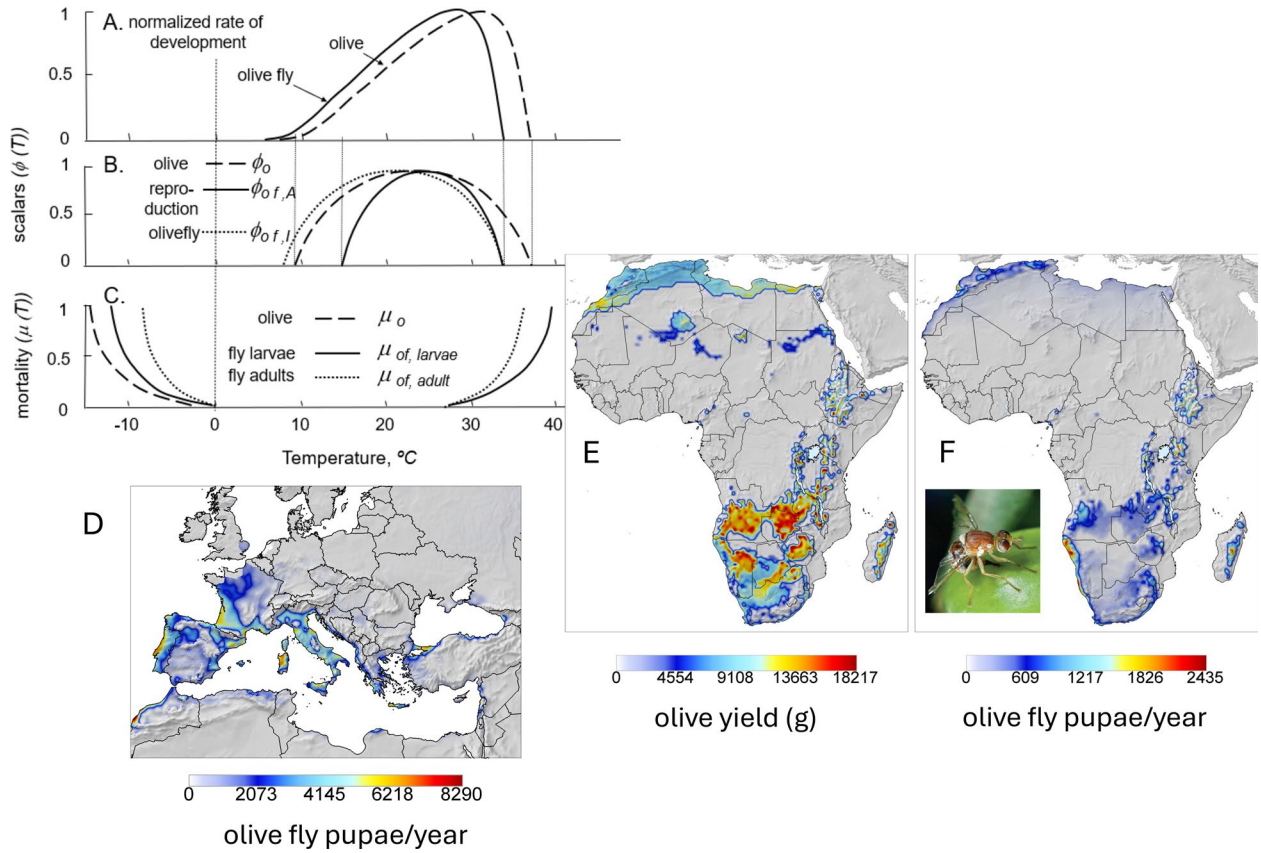

Fig. 8 Olive and olive fly: biodemographic functions for olive and olive fly (**A**–**C**, [10]), **D** the prospective distribution of olive fly in the Mediterranean Basin, and the prospective distribution in Africa of (**E**) relative olive yield and (**F**) of olive fly above 500 mm annual rainfall. Note that olive is cultivated in Egypt and other regions of North Africa under irrigation

hyperparasitoid *Acroclisoides sinicus* (Huang and Liao), and a tachinid parasitoid fly of the genus *Trichopoda* spp. that attacks large nymphs and adults (Fig. 9A, B). The BDFs for BMSB are summarized in Fig. 9C and in Gutierrez et al. [63] for the other species.

The prospective range of BMSB is wide throughout temperate areas of Europe, and Mediterranean coastal areas from Morocco across to Egypt (Fig. 9D). BMSB is limited by extreme cold temperatures northward in Europe and by hot weather in southern areas. Prospectively, most of the African continent is unfavorable for BMSB with favorability predicted in coastal North Africa and the tip of South Africa (Fig. 9E). In sharp contrast, Yonow et al. [64] used the SDM algorithm CLIMEX [65] to predict the global distribution of BMSB and the two egg parasitoids, with a predicted wide distribution in sub-Saharan Africa.

(4) Tomato pinworm

The invasive stenophagous tomato pinworm (*Tuta absoluta* Meyrick (Lepidoptera: Gelechiidae)) is a destructive pest of solanaceous crops. The pinworm is native to the cooler climes of Peru but has extended its geographic range to sub-tropical areas of Brazil. After its initial detection in Spain in 2006, its invasiveness in the Palearctic was analyzed in 2010 and 2019 (see [49]) using CLIMEX and posited that only coastal southern Europe would be suitable for the pest. This occurred, because the projections were based on its known range expansion in South America into tomato-growing areas with warm climates akin to coastal Mediterranean areas. The analyses failed to consider that the pest originated in the cold semi-arid climes of the Andean highlands, and hence the geographic range of the pinworm in Europe proved to be much greater (Fig. 10F). Its full global invasive potential was not identified until rapid colonization of large areas of Europe had occurred (see [49]), followed by Africa and parts of Asia, where it has become a major food security problem.

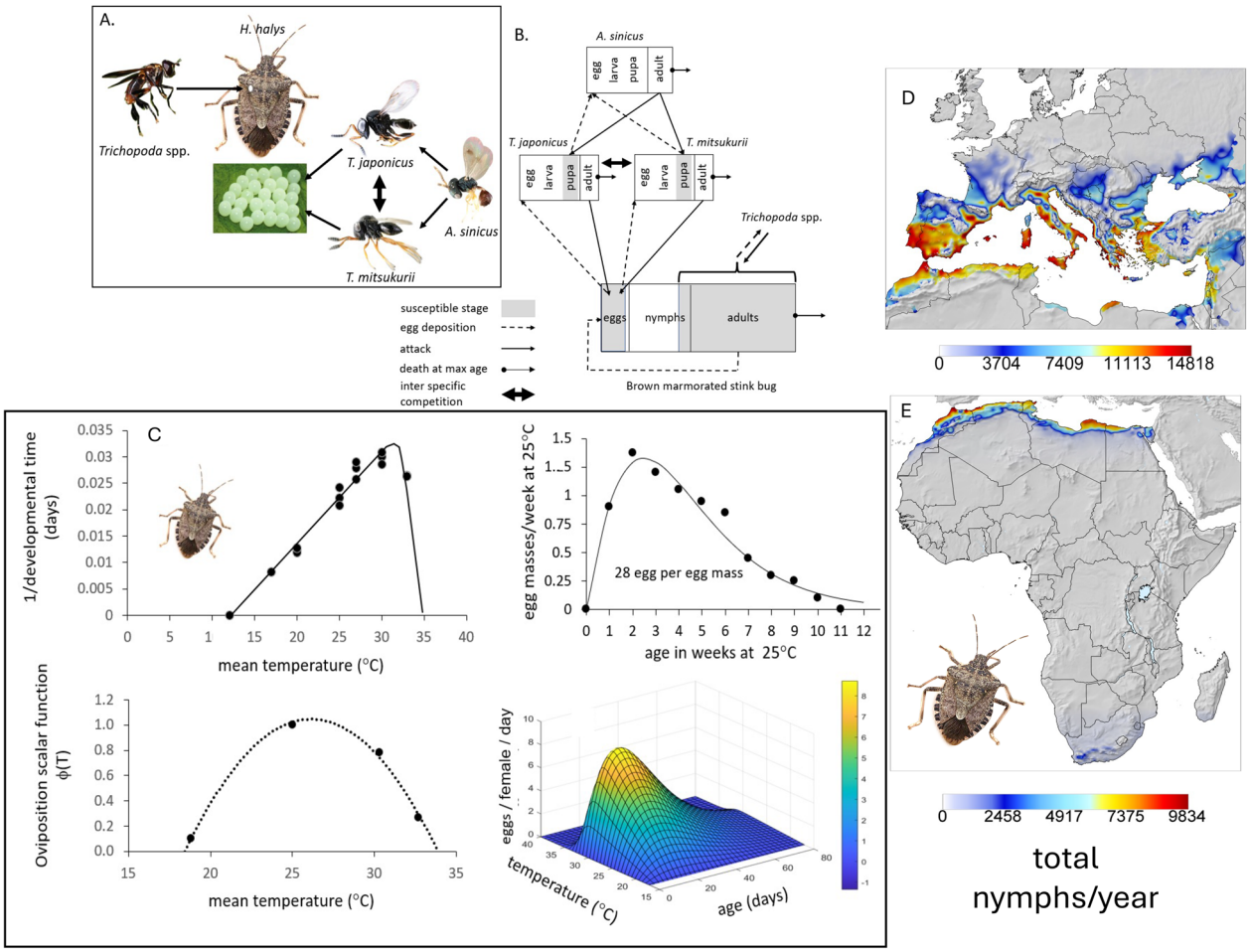

Fig. 9 Asian brown marmorated stink bug (BMSB): **A** the trophic relationships, **B** age specific attack relationships, **C** biodemographic functions for BMSB (see [63] for BDFs of the other species), and **D** the prospective distribution and average relative abundance (i.e., invasiveness) of BMSB nymphs in Palearctic–Mediterranean Region (modified from [63]) and **E** in Africa

The BDFs for tomato pinworm are illustrated in Fig. 10A–D. Its lower thermal threshold is 7.9 °C with an upper thermal threshold of ~ 35 °C, oviposition occurs in the range 7.9–32 °C, the optimal temperature for maximum oviposition is ~ 27.5 °C, and it has a weak pupal diapause [67]. The mortality rates across temperatures (μ_T(T)) were estimated from data in the literature [67–71] (Fig. 10E) indicating the moth is tolerant to moderately cold and high temperatures (Fig. 10F; see [49]).

The prospective invasive distribution of *T. absoluta* in Africa includes the cooler climes of Senegal, Morocco across coastal North Africa to Egypt and the Levant, with highest populations in sub-tropical and tropical Africa, with decreasing levels in temperate regions of South Africa (Fig. 10G).

(5) False codling moth

The polyphagous false codling moth (FCM, *Thaumatotibia leucotreta* (Meyrick) (Lepidoptera: Tortricidae)) is native to Africa with an endemic range in Kenya–Ethiopia across sub-Saharan Africa to West Africa, with a range extension as an invasive species into South Africa. Numerous detections have occurred in Europe on cut flowers imported from East Africa, and its invasive potential was assessed using a PBDM [72].

Data on FCM biology is mostly from South Africa, where it is an invasive species (Fig. 11A–G, see [73–77] and others) and suggests it is adapted to a range of temperatures between 10 and 35 °C with the optimum near 24–25 °C. The lower threshold for FCM larval and pupal development is ~ 10.5 °C with an upper threshold

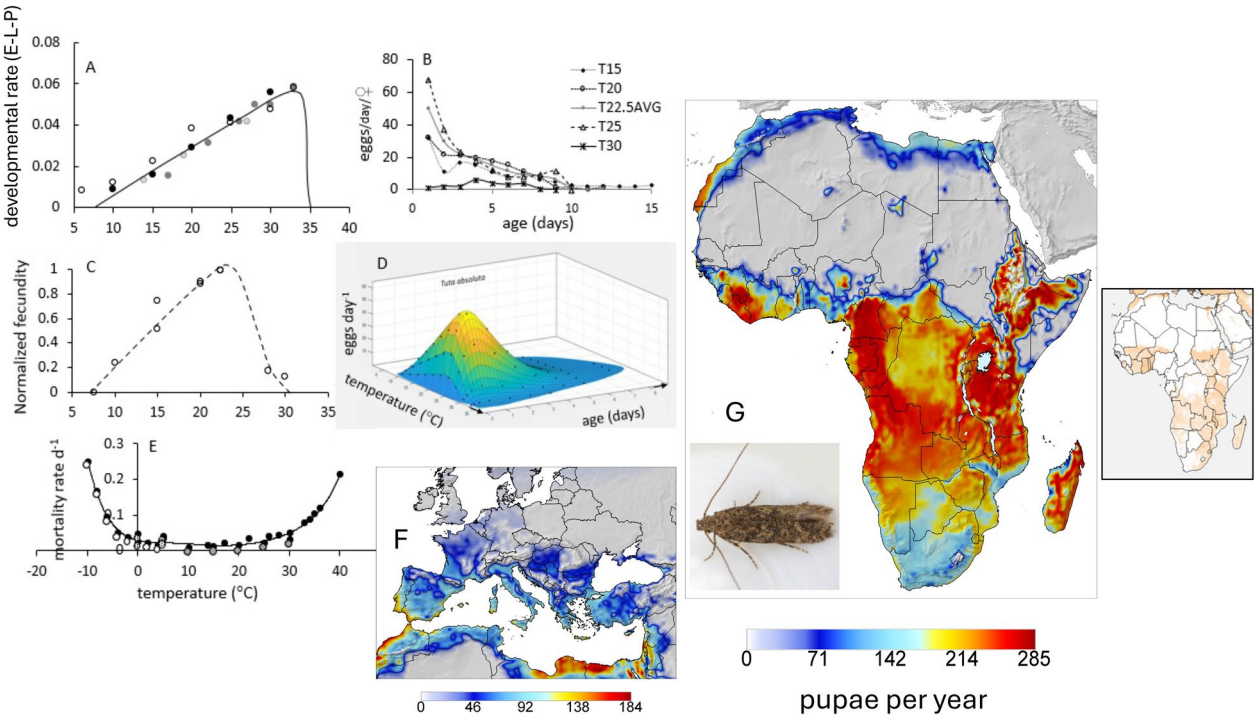

Fig. 10 Tomato pinworm: biodemographic functions (**A**–**E**), and prospective distribution and average relative abundance in (**F**) the Palearctic–Mediterranean Region [49], and (**G**) in Africa using 2005–2010 weather. The inset in G is the distribution of tomato cultivation (see [66])

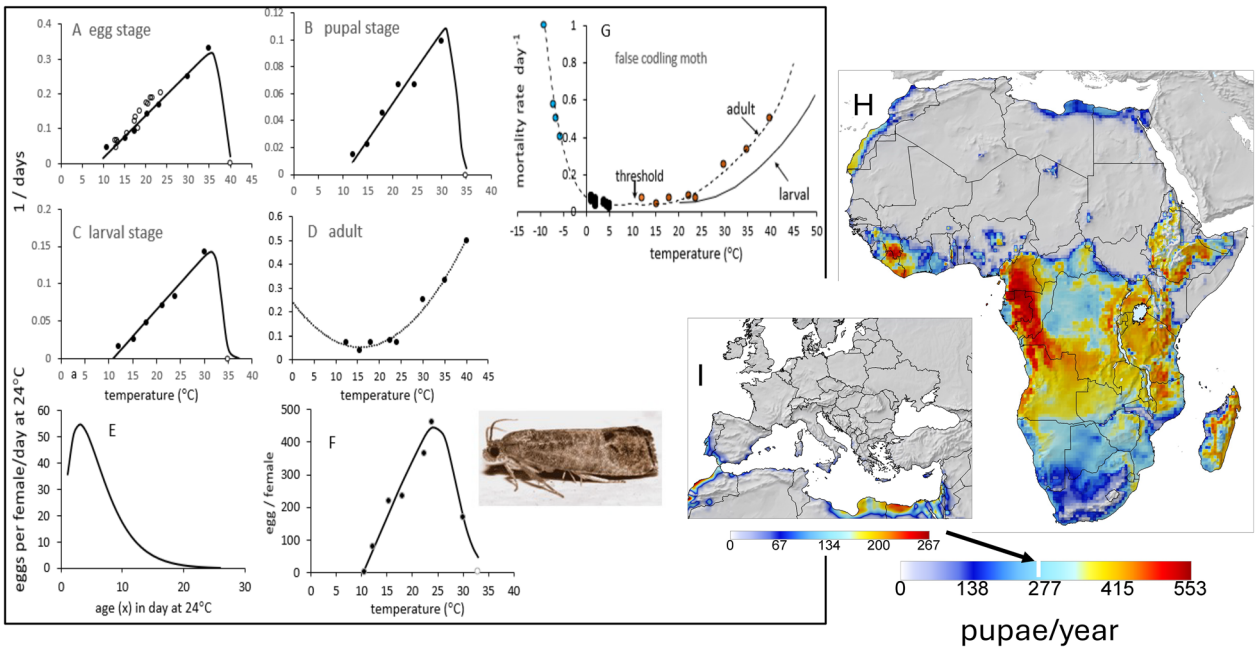

Fig. 11 False codling moth: biodemographic functions (**A**–**G**), and prospective distribution and average relative abundance of pupae in Africa (**H**) and in the Palearctic–Mediterranean Region (**I**) (see [72])

of ~ 30 °C, females have a short preoviposition period of 0.5–1.5 days at 25 °C and lay eggs singly. Average fecundity increases rapidly above ~ 11 °C with a sharp decline above ~ 26 °C to zero at ~ 33 °C. The moth lacks a diapause stage, and the available temperature-dependent mortality data suggest the larval stage is intolerant of

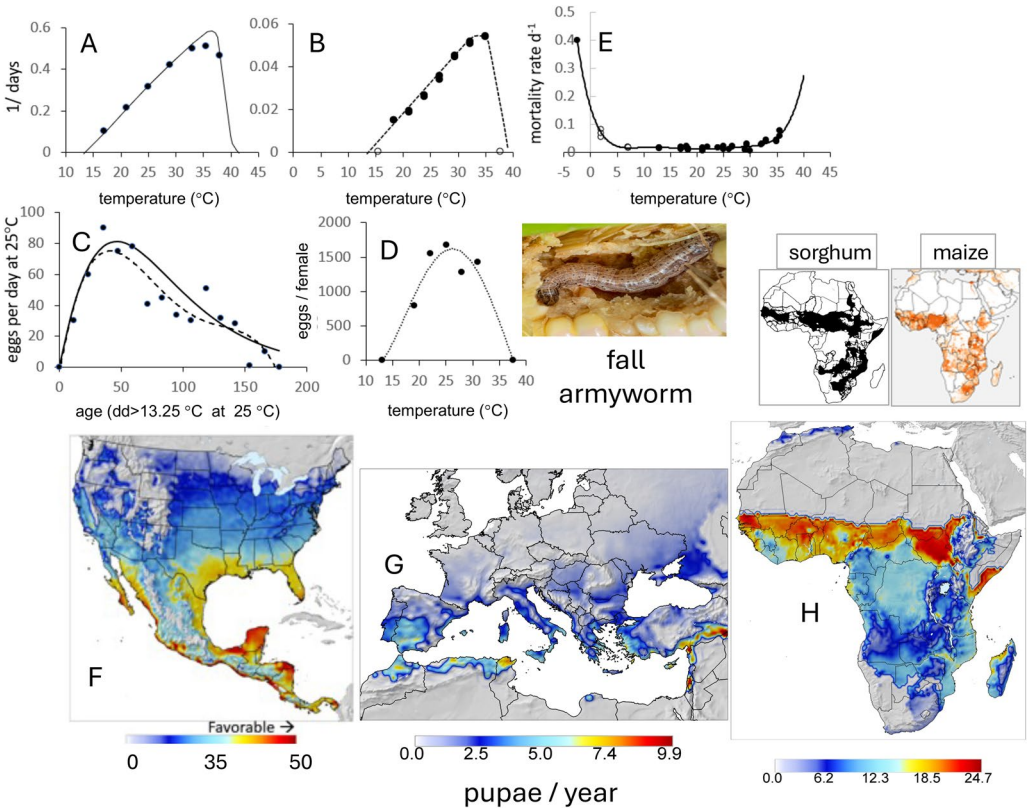

Fig. 12 Fall armyworm: **A**–**E** biodemographic functions (e.g., [80, 81], and others), and using 2000–2010 weather the prospective distribution and average relative abundance of pupae in (**F**) North and Central America, **G** the Palearctic–Mediterranean Region, and (**H**) Africa. The insets above 12H are the distribution of sorghum and maize in Africa [66]. Map 12H is masked at > 400 mm annual rainfall

freezing temperatures. However, larvae are more tolerant to high temperatures than the adult stage [77], and this difference is captured by a 4 °C higher displacement of larval vs. adult mortality rates above 24 °C (i.e., the solid line in Fig. 11G).

The false codling moth has a documented wide distribution in areas of sub-tropical and tropical Africa (Fig. 11H), but its prospective distribution in Mediterranean areas is restricted to south coastal Iberian Peninsula and north coastal Africa (Fig. 11I).

(6) Fall armyworm

The polyphagous fall armyworm (FAW, *Spodoptera frugiperda* J.E. Smith (Lepidoptera: Noctuidae)) is native to subtropical–tropical regions of the Americas, has a high migratory capacity, lacks a diapause stage, and has a female-biased sex ratio. The moth was first reported in Africa from Nigeria in 2016 [78] and is now established across Africa, where it causes extensive damage to basic staple crops, such as maize and sorghum (see [79]).

The BDFs for FAW are illustrated in Fig. 12A–D showing the larvae and pupae stages have a high lower thermal threshold (12.95 °C, 13.25 °C, respectively) and a relatively high upper thermal threshold of 37.7 °C. In the model, the larval threshold is used for the egg and adult stages. At ~ 25 °C, female moths may produce more than 1000 eggs over a 14.5-day period, but fecundity is zero at 13 °C and 37.5 °C. The moth is cold intolerant but survives well at high temperatures (Fig. 12E), and it is relatively insensitive to changes in relative humidity (see [80, 81]).

In North America, the prospective permanent distribution of FAW is sub-tropical and tropical areas, with the limits to permanent overwintering being above the midpoint of its prospective density range as mapped in Fig. 12F. The literature suggests the moth can migrate hundreds of miles on winds that during spring and summer in the USA flow strongly northward carrying moth adults as far as eastern Canada. This allows transient populations to develop in areas of North America, where winter temperatures limit year around survival.

Masking areas with less than 400 mm annual precipitation, shows that FAW has low capacity to establish in warmer areas of Europe (Fig. 12G) confirming PBDM results of Gilioli et al. [82, 83]. Prospectively, only low

populations are predicted in northern Algeria and Tunisia, with higher populations predicted in the Levant. The prospective geographic distribution and relative abundance of FAW in Sub-Saharan Africa is a broad band across the continent from Senegal to Somalia–Uganda–Kenya (Fig. 12H) with prospective maximum densities ~ 50% lower than in its native range in Mexico and Central America (12F vs. 12H). The distribution of maize and sorghum cultivation in Africa is shown as insets in Fig. 12H [66], and as is the case in North America, the geographic range of favorability is greater for maize and sorghum than for FAW.

Linkages of FAW to maize and sorghum as has occurred for cotton [84], and GIS layers for their distribution in Africa would improve the region-wide simulations for use in management and policy development.

(7) Citrus/citrus psyllid/parasitoid/greening disease system.

The invasive Asian citrus psyllid (ACP, *Diaphorina citri* Kuwayama (Hemiptera: Liviidae) is a destructive pest causing damage to citrus and to species in 25 genera of Rutaceae [85, 86]. The psyllid is reported from tropical and subtropical Asia (see [86]), tropical islands (Reunion, Guadeloupe, Mauritius), parts of South and Central America, Mexico, and the Caribbean [85, 87, 88]. ACP was first detected in Florida in 1998 [89, 90], in Texas in 2000 [91], and in southern California in 2008, where there is concern it will spread northward along the coast and into the Great Central Valley [92, 93]. ACP has been found in Benin and Nigeria in West Africa and in Kenya, Uganda, and Tanzania in East Africa [94]. Its prospective distribution is similar to that of the African citrus psyllid (*Trioza erytreae* (Del Guercio) (see [95, 96]).

A PBDM system model was developed to assess prospectively the geographic distribution and relative yield of citrus (a generic model), the relative densities of the ACP, and its potential control by the parasitoid (*Tamarixia radiata* Waterston) and native predators in North America and the Mediterranean Basin [97]. Also included in the study was an estimate of the prospective severity of citrus greening disease. The PBDMs are used here to assess areas of favorability for the species across Africa. The PBDMs for citrus and the psyllid are MP-based, that of the parasitoid is BDF-based, and the model for citrus greening disease is an empirical concave function of temperature.

The upper and lower thermal thresholds of ACP are 12.85 and 35.5 °C, respectively, with the developmental rate declining to zero above ~ 31 °C. The lower thermal threshold for oviposition is about 16 °C, the optimum is 31 °C and the maximum is about 40 °C (box Fig. 13Aa–Ac). ACP overwinters as an adult but is relatively cold susceptible with the mortality rate d^{-1} being unity at a mean of − 2.5 °C (estimated from hourly rates in Fig. 13Ad). The upper and lower thermal threshold of *T. radiata* are 7.5 and 35.5 °C, respectively, with the developmental rate declining to zero above ~ 31 °C, with the lower thermal threshold for oviposition of ~ 12 °C, an optimum at 26 °C and the maximum of ~ 37 °C (box Fig. 13Ba–Bc). The psyllid's vital rates are those of a subtropical–tropical species, while those of *T. radiata* are more temperate.

Absent natural control, the potential distribution of ACP is pan-African with the highest densities predicted in tropical and subtropical areas of Africa (not shown). The strain of *T. radiata* in our model is from Brazil, and prospectively would not change the distribution of the psyllid (Fig. 13C) nor would it provide effective biological control in Africa as it decreases ACP densities ~ 50% (Fig. 13D, E).

ACP is a vector of the bacterial pathogen ('*Candidatus Liberibacter asiaticus* (CLas)), the causal agent of citrus greening disease (Huanglongbing disease (HLB)) in citrus in many areas of the world. ACP also vectors two other related phloem-inhabiting fastidious bacteria: *Candidatus Liberibacter africanus* (CLaf) and *Ca. Liberibacter americanus* (CLam) (see [95]). The diseases are also transmitted to other trees via clonal propagation and grafting of infected material, with the endemic African citrus psyllid being the primary vector of CLaf in Africa [95]. Citrus greening disease was recorded in Brazil in 2004 [98], in south Florida in 2005 [99], and in southern California in 2008 ([92], http://cisr.ucr.edu/Asian_citrus_psyllid. html.). Greening disease has wider thermal tolerances than the psyllids, and this is reflected in the prospective wider geographic distribution of the normalized disease severity index across tropical Africa (Fig. 13F).

A GIS layer for the distribution of Rutaceous hosts including citrus in Africa would help define the limits of ACP and HLB. Furthermore, greater physiological detail for citrus growth and development and greening diseases would improve the model. We note that the model can be easily adapted for the African citrus psyllid.

(8, 9) Invasive mosquitoes—*Aedes albopictus* (Skuse, 1894) and *Aedes aegypti* (L.) (Diptera: Culicidae)

Ae. albopictus is an aggressive human-biting mosquito that is a major vector of arbovirus diseases including dengue, Zika, and chikungunya, while *Ae. aegypti* vectors yellow fever, dengue, chikungunya, Zika, Mayaro, and other viral disease agents. A white band on the thorax of *Ae. albopictus* readily distinguishes it from *Ae. aegypti*.

Aedes larvae develop in standing water in nature and in artificial containers in urban areas. The lower thermal

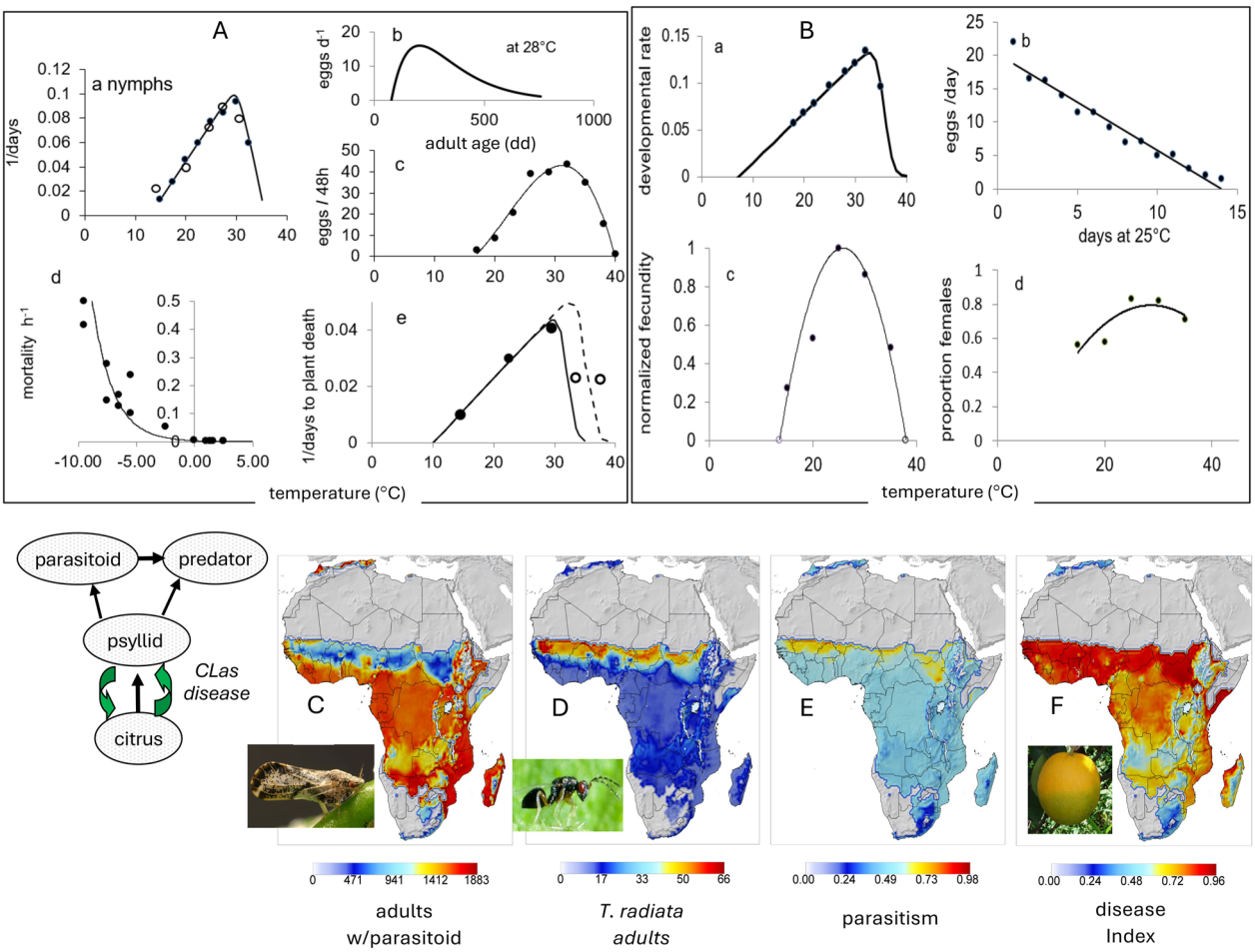

Fig. 13 Citrus/Asian citrus psyllid (ACP)/parasitoid/predator/greening disease system (see [97]) with maps masked > 400 mm rainfall: **A** biodemographic functions for ACP {(Aa) developmental rate, (Ab) oviposition profile per day at 28 °C on age in degree days, (Ac) eggs per 48 h on temperature, (Ad) mortality rate per hour on temperature, (Ae) rate of infected plant death on temperature}, **B** biodemographic functions for *T. radiata* {(Ba) developmental rate on temperature, (Bb) oviposition per day at 25 °C, (Bc) normalized eggs per day on temperature, (Bd) proportion females on temperature, and the prospective distribution and average relative abundance (**C**) of ACP adults/year/tree with parasitism and low predation by indigenous species, (**D**) *T. radiata* adults, **E** prospective average parasitism rate of nymphs, **F** greening disease index (see [95])

thresholds of *Ae. albopictus* and *Ae aegypti* larvae are 10.5 °C and 12 °C, respectively, but the upper inflection points, where the developmental rate begins to decline to zero is ~ 32.5 °C for *Ae. albopictus* and ~ 36 °C for *Ae. aegypti* (Figs. 14A, 15A; [100–108]). The effects of vapor pressure deficit ($0 \le \phi_{VPD} \le 1$) was used to scale oviposition during dry periods in both species. Egg diapause is present in *Ae. albopictus* but not in *Ae. Aegypti* [109–112] that with its low egg developmental threshold enables *Ae. albopictus* to persist and expand its range into temperate regions [113]. Diapausing *Ae. albopictus* eggs are genetically programmed to environmental change (e.g., photoperiod) which precedes the onset of unfavorable cooler conditions. During diapause, *Ae. albopictus* eggs remains dormant and refractory to environmental stimuli [108, 110, 114, 115], but readily hatch when favorable photoperiod, moisture and temperature conditions return.

Quiescence during dry periods occurs in the egg stage of both *Ae. albopictus* and *Ae. aegypti* when the formed embryo (pharate larvae) receives an external stimulus such as a sudden decrease in humidity and/or a sharp increase in temperature signaling unfavorable conditions for successful hatching. When favorable conditions return, quiescent embryos are sensitive to contact with water that induces rapid hatching [109, 111, 116, 117].

The prospective distribution of *Ae. albopictus* in temperate regions of the Mediterranean Basin are illustrated in Fig. 14B confirming PBDM predictions of Pasquali et al. [119]. Our model predicts the high invasive potential of *Ae. albopictus* in tropical Mexico, lower invasive

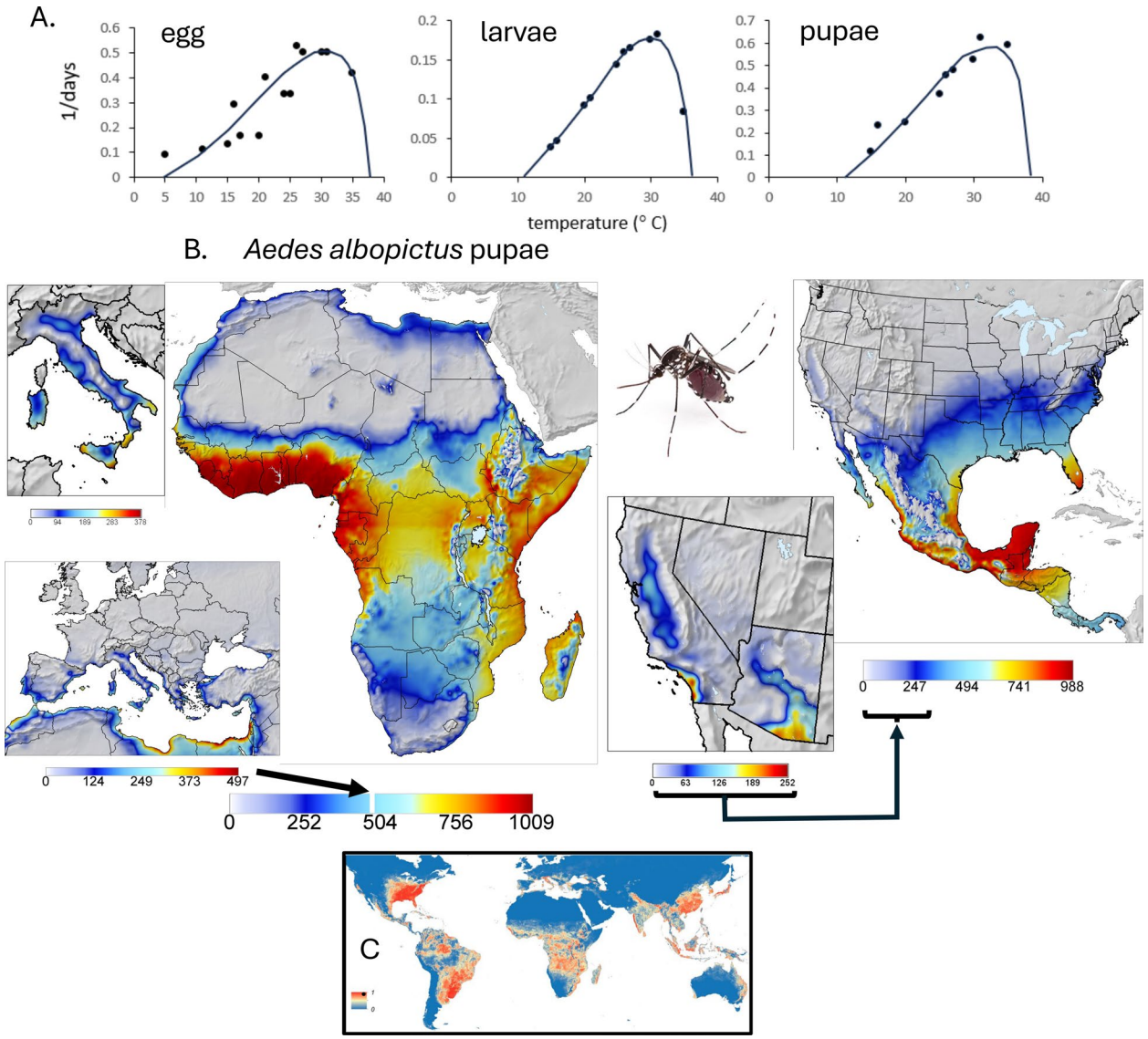

Fig. 14 *Aedes albopictus*: **A** egg, larval and pupal developmental rates on temperature, **B** prospective distribution and average relative abundance in the Palearctic–Mediterranean Region, Africa, and California–Arizona with SDM predictions of mosquito distribution in box (**C**) from Kraemer et al. [118]. The illustration of a female *Ae. albopictus* is from https://www.wechu.org/z-health-topics/aedes-albopictus-mosquito

potential in warmer temperate regions of the SE USA, and still lower levels in Coastal southern California and the hot Great Central Valley of California.

Prospectively, *Ae. aegypti* cannot invade temperate regions of Europe or the Mediterranean Basin and, compared to *Ae. albopictus* has lower populations levels in Mexico and Central America, and in hot regions of California and Arizona (Fig. 15B).

The simulated prospective distributions of the two species across Africa are similar (Figs. 14B vs. 15B), but the abundance of *Ae. albopictus* is greater than *Ae. aegypti* in favorable regions. This difference is illustrated as the ratio of cumulative annual pupae ((*Ae. Albopictus–Ae. aegypti*)/*Ae. aegypti*) (Fig. 16). Also shown in the figure is the limited distribution of both species in arid regions of Africa.

Using presence data and an ensemble Boosted Regression Tree (BRT) approach, Kraemer et al. [118] mapped the global favorability distributions of *Ae. albopictus* and *Ae. aegypti*. They found the distribution of *Ae. albopictus* is sub-tropical and tropical with range extensions into temperate regions (Fig. 14C), while the distribution of *Ae. aegypti* is sub-tropical and tropical (Fig. 15C).

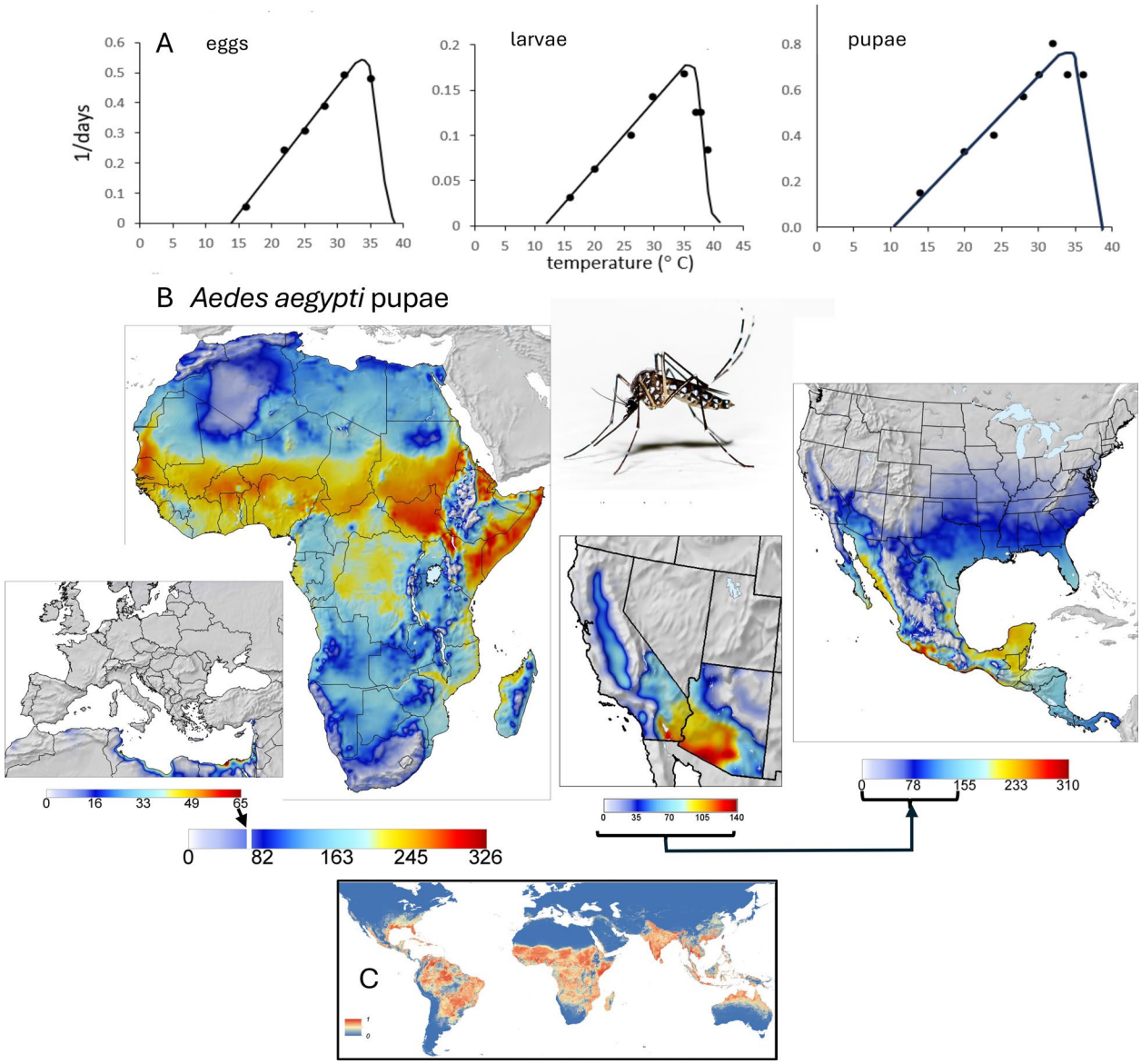

Fig. 15 *Aedes aegypti*: **A** egg, larval and pupal developmental rates on temperature, **B** prospective distribution and average relative abundance in the Palearctic–Mediterranean Region, Africa, and California–Arizona. SDM predictions of global mosquito distribution in box (**C**) are from Kraemer et al. [118]. The illustration of *Ae. aegypti* is from https://www.theatlantic.com/science/archive/2021/06/dengue-mosquitoes-defanged/619161/

A major deficiency of our models is that *Aedes* mosquitoes require standing water to breed, and this factor was not included in our model, but this could be corrected by a water balance model without changing the basic structure of the model. Rainfall and *VPD* were used as surrogates. Despite this, the PBDM maps for both species compare well with the SDM predictions of Kraemer et al. [118]. Furthermore, PBDMs allow incorporation of new findings on the biology and physiology of the species that would improve the models capacity for assessing population phenology and relative density useful for regional assessment of population suppression techniques such as cytoplasmic incompatibility based on *Wolbachia* endosymbionts [120].

(10–13) Four invasive fruit fly species

Sub-tropical and tropical fruit flies are among the most economically important invasive species and are frequently detected by quarantine services in temperate areas. Detection often triggers quarantine and eradication programs conducted without a holistic understanding of the threat posed. A single eradication

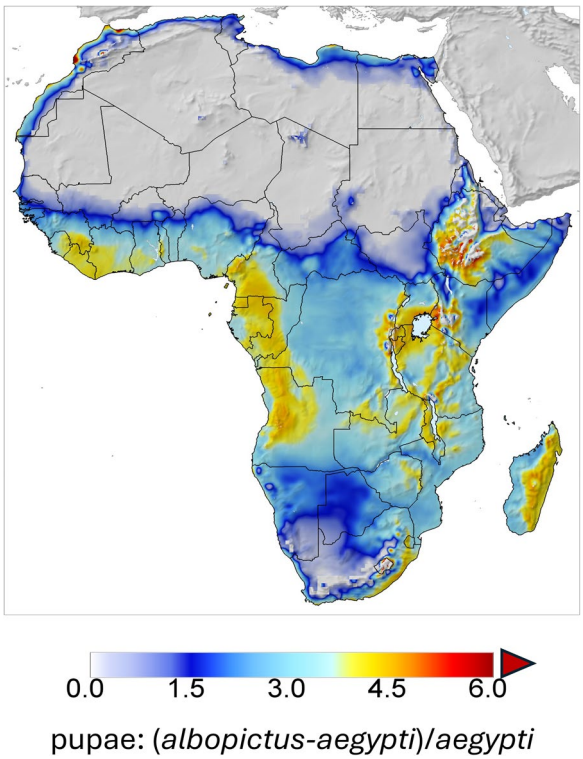

Fig. 16 Ratio of pupal densities ((*Ae. Albopictus–Ae. aegypti*)/ *Ae. aegypti*) across Africa masked at 6. The lattice cell values are averages for the 10-year period 2001–2010

campaign against tropical fruit flies in the USA costs approximately US$32 million, and up to US$100 million as occurred for medfly in California during 1980–81 [121]. Hence, determining the favorability of invaded temperate areas for tropical fruit flies under extant weather and under climate change is critical for policy development [121].

The most economically important invasive fruit flies are in the family Tephritidae: Diptera from four genera: *Ceratitis, Anastrepha, Bactrocera* and *Rhagoletis*. Tephritid flies have had considerable success in invading new tropical and sub-tropical regions of the world, but less so in temperate regions [121]. Their success is attributed to wide host ranges and possibly developmental responses and tolerance to environmental variables through phenotypic plasticity and selections (e.g., [122]).

Weather-driven PBDMs of the biology and dynamics of four sub-tropical and tropical species (Mediterranean fruit fly (*Ceratitis capitata*; medfly) from East Africa, melon fly (*Bactrocera cucurbitae*) native to India, Oriental fruit fly (*Bactrocera dorsalis*) from Asia, and the Mexican fruit fly (*Anastrepha ludens*; mexfly) were used to estimate prospectively their geographic range and relative abundance (i.e., invasive potential) in North and Central America, and in the European–Mediterranean region under extant and climate change weather (see [121]). The BDFs for the four species are compared in Fig. 17A–E. The BDFs for olive fly (*Bactrocera oleae* (see Fig. 8)) and spotted winged fruit fly (*Drosophila suzukii* (Matsumura) (Drosophilidae)) [123] that successfully invaded temperate regions, are also included in Fig. 17A–E to illustrate the relative displacements of their BDFs relative to those of the four sub-tropical–tropical species.

Only a brief review of the biology of the four species is reported here (see [121]). Medfly is native to sub-Saharan Africa and has spread throughout the Mediterranean region, southern Europe, the Middle East, Western Australia, South and Central America, and Hawaii. Mexfly is native to Mexico and Central America. Oriental fruit fly and melon fly are found in tropical regions of the Eastern Hemisphere. None of the four species has a diapause stage and hence cold weather is an important factor restricting their geographic range in temperate regions. Temperature and low relative humidity may affect fruit fly reproduction, survival, and permanence in seemingly favorable areas [121].

Prospective distribution maps of the four fruit flies in Africa are shown in Fig. 17F–I. The distribution of Mediterranean fruit fly and Mexican fruit fly across Africa are similar, with the Mexican fruit fly prospectively being ~ 25% more abundant in favorable areas of Africa (Fig. 17F, G) suggesting it could be an important invasive species in sub-Saharan Africa. Melon fly attacks more than 125 vegetable species, including tomato, while Oriental fruit fly attacks a very wide variety of fruits, with avocado, mango, and papaya being attacked the most. Both species have similar prospective distributions, with Oriental fruit fly being ~ 60% more abundant (Fig. 17H, I). The distribution of melon fly has been masked for the distribution of tomato to illustrate potential host effects. The vertical bars in the sub-figures are visual comparisons of maximum densities of the four species indicating Oriental fruit fly would be the most abundant in Africa.

The PBDMs could benefit from improved estimates of the effects of relative humidity (or VPD) on species vital rates. As demonstrated for olive fly, linkage to plant hosts in the model and GIS layers of the major hosts for each of the fruit fly species would enhance mapping their geographic range.

Discussion

Most agroecosystems studies are not holistic, often lack cohesive scientific underpinnings, and are studies with limited generality. What is required to resolve this conundrum is the development of analytical methods (models) that capture the underlying biology and dynamics of the species and species interactions as driven by weather

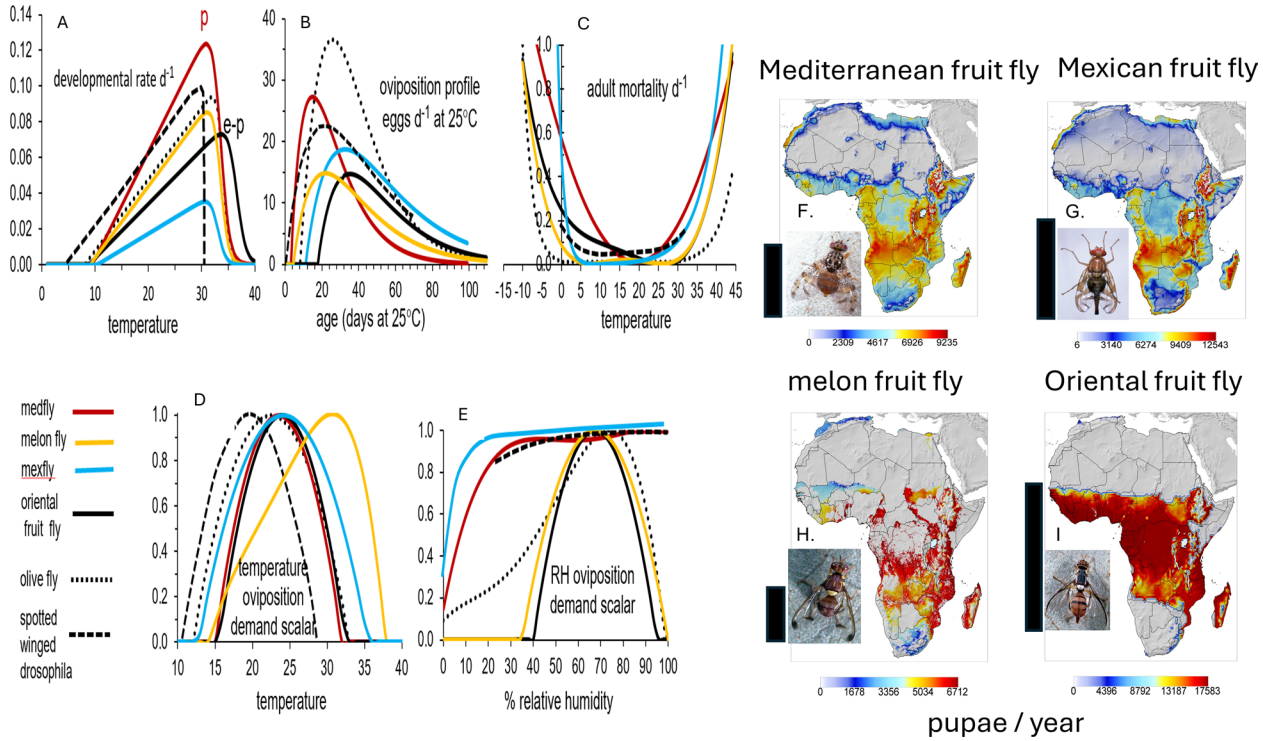

Fig. 17 Four invasive fruit flies: biodemographic functions (**A**–**E**) (see [121] for details), and prospective distribution and average relative abundance in Africa of (**F**) Mediterranean fruit fly, **G** Mexican fruit fly, **H** melon fly masked for the distribution of tomato, and **I** Oriental fruit fly masked annual rainfall > 500 mm. (Photos of fruit fly adults are courtesy of Jack Kelly Clark, University of California Statewide IPM Program)

and resource levels; models that can be libraries, where new findings may be added to refine understanding and predictions. We must recognize that studies of agroecological problems are exercises in applied population ecology; of crop plants, pests, and natural enemy dynamics as driven by weather and edaphic, agronomic, and economic factors. Furthermore, climate change is simply another weather scenario with potentially disastrous consequences for species establishment and impact. Mechanistic models of the biology of species and of their interactions enable addressing some of these issues.

The very large task of modeling thirteen invasive (and associated) species was to show how the same model structure could be used to develop physiologically based demographic models (PBDMs) of poikilotherm species dynamics and species interactions as driven by weather, and to prospectively map their geographic distribution and relative abundance (i.e., our metrics of invasiveness) based on their discerned biology. PBDM bridge some of the gaps between field ecology, demography and physiology and augment SDM analyses. PBDMs may be parameterized as bioeconomic models of how organisms acquire and allocate energy/dry matter (i.e., metabolic pool (MP)) or may be parameterized using biodemographic functions (BDFs) that summarize the vital rates estimated from age-specific life table studies conducted under an array of temperatures, relative humidity, levels of nutrition, and other factors. A unifying notion is that BDFs are the net outcomes of MP energy/resource acquisition and allocation processes under the experimental conditions. This biology can be used to capture the weather and resource driven dynamics in distributed-maturation time population models. In sum, PBDMs are time varying life tables.

The development of PBDMs is deemed difficult [124], but this is not the case as demonstrated here for thirteen invasive species (actually 20) described using the same relatively simple model structure. However, as a caveat, we note that all models are incomplete including the PBDMs presented here based largely on data from the literature, that no model can be a one-to-one description of the biology. We stress the need for sound biological data and note that PBDMs streamline identification and collection of the data [8, 125] and easily accommodate additional biology and physiology to refine the model without changing its basic character or structure. Our goal was to capture the key features of the biology of the species sufficient to yield sound predictions about

their weather-driven dynamics independent of presence records sufficient to predict their distribution and relative abundance in a GIS context across the vast geographic region of Africa. Where available, the prospective geographic distributions predicted by our model were referenced to predictions of SDMs, with only the predictions for the potential distribution of the Asian stinkbug *H. halys* in Africa using the CLIMEX algorithm (see [64]) being strongly at odds with our assessment.

In developing PBDMs, we must consider that invasive species with wide native geographic distributions across diverse ecological zones may have region-specific strains that have different behavioral and physiological traits, and that the invasive inoculum invading a novel environment may come from any part of that range. The biological parameters of the inoculum strain may determine its establishment success, temporal dynamics, and adaptation to the new environment. Hence, capturing the biology of species/strain does matter in real-world applications. We note that in PBDMs, strain attributes are parameter differences (e.g., [126]).

PBDMs are heuristic tools to guide data collection to increase scientific understanding, and if complete enough may be used for the development of management practices and policies. Three recent holistic PBDM analyses are those of Indian hybrid Bt cotton [21], the invasive tomato pinworm [49], and Colombian coffee [20] that explained the important biological components of the system and provided real-world management recommendations. Furthermore, holistic PBDMs can be used as the objective function in economic analyses to provide important insights not amenable to econometric analyses of field panel data [21, 23, 24], and in reduced form to examine ecological theory [127]. We strongly caution that no model, including PBDMs, can predict crop yield or pest organism densities and damage with a sufficient degree of accuracy for economic speculation.

Numerous PBDMs have been developed and implemented, some in a GIS context (Supplemental Materials Table 1), using in-house heritage software based on the methods outlined in our text (see [7, 8]). However, transferring PBDM development capacity to researchers widely has proven difficult because of conceptual leaps and a dearth of enabling software. To this end, a general PBDM/GIS Web platform is under development with the goal of enabling non-experts to construct PBDMs for various purposes at local, regional, and larger scales (Supplemental Materials Fig. 1) with the strong caution for the need of sound biological data and restraint in interpreting the result.

Supplementary Information

The online version contains supplementary material available at https://doi.org/10.1186/s12302-025-01084-y.

Supplementary material 1.

Acknowledgements
We continue to be grateful to the international network for maintaining the Geographic Resources Analysis Support System (GRASS) software and making it available to the scientific community. The study was supported by CASAS Global NGO (https://www.casasglobal.org), the McKnight Foundation (grant number 22-341 and 24-124), and project TEBAKA (project ID: ARS01_00815) co-funded by the European Union—ERDF and ESF, "PON Ricerca e Innovazione 2014-2020". Access to the library search engine of the University of California at Berkeley was invaluable.

Author contributions
All authors contributed equally.

Funding
The study was supported by CASAS Global NGO (https://www.casasglobal.org), the McKnight Foundation (grant number 22–341 and 24–124), and project TEBAKA (project ID: ARS01_00815) co-funded by the European Union—ERDF and ESF, "PON Ricerca e Innovazione 2014–2020".

Availability of data and materials
No data sets were generated or analysed during the current study.

Declarations

Ethics approval and consent to participate
Not applicable.

Consent for publication
Not applicable.

Competing interests
The authors declare no competing interests.

Author details
[1]Center for the Analysis of Sustainable Agroecological Systems, Kensington, CA 94707, USA. [2]College of Natural Resources, University of California, Berkeley, CA 94720-3114, USA. [3]Agenzia Nazionale per le Nuove Tecnologie, l'Energia e lo Sviluppo Economico Sostenibile (ENEA), Centro Ricerche Casaccia, Via Anguillarese 301, 00123 Rome, Italy. [4]mundialis GmbH & Co. KG, Koelnstrasse 99, 53111 Bonn, Germany. [5]Andora Cloud, Via Alghero 4, 09045 Quartu Sant'Elena, Italy. [6]Facultad de Ciencias Básicas y Aplicadas, Universidad Militar Nueva Granada, Cr. No. 101-17 80, Bogotá, Colombia. [7]IDEMS International, Reading, Berkshire, UK.

Received: 24 September 2024 Accepted: 20 February 2025
Published online: 29 April 2025

References

1. Cuthbert RN, Diagne C, Hudgins EJ et al (2022) Biological invasion costs reveal insufficient proactive management worldwide. Sci Total Environ 819:153404. https://doi.org/10.1016/j.scitotenv.2022.153404
2. Pimentel D, Lach L, Zuniga R, Morrison D (2000) Environmental and economic costs of nonindigenous species in the United States. Bioscience 50:53–65. https://doi.org/10.1641/0006-3568(2000)050[0053:EAECON]2.3.CO;2
3. Henry M, Leung B, Cuthbert RN et al (2023) Unveiling the hidden economic toll of biological invasions in the European Union. Environ Sci Eur 35:43. https://doi.org/10.1186/s12302-023-00750-3

4. Pyšek P, Richardson DM, Pergl J et al (2008) Geographical and taxonomic biases in invasion ecology. Trends Ecol Evol 23:237–244. https://doi.org/10.1016/j.tree.2008.02.002
5. Khuroo AA, Reshi ZA, Rashid I, Dar GH (2011) Towards an integrated research framework and policy agenda on biological invasions in the developing world: a case-study of India. Environ Res 111:999–1006. https://doi.org/10.1016/j.envres.2011.02.011
6. Elith J (2017) Predicting distributions of invasive species. In: Robinson AP, Walshe T, Burgman MA, Nunn M (eds) Invasive species. Cambridge University Press, Cambridge, pp 93–129
7. Gutierrez AP (1996) Applied population ecology: a supply-demand approach. John Wiley and Sons, New York
8. Gutierrez AP, Ponti L (2013) Eradication of invasive species: why the biology matters. Environ Entomol 42:395–411. https://doi.org/10.1603/EN12018
9. Gutierrez AP, Baumgärtner JU (1984) Multitrophic level models of predator-prey energetics: I. Age-specific energetics models - pea aphid *Acyrthosiphon pisum* (Homoptera: Aphididae) as an example. Can Entomol 116:924–932. https://doi.org/10.4039/Ent116923-7
10. Gutierrez AP, Ponti L, Cossu QA (2009) Effects of climate warming on olive and olive fly (*Bactrocera oleae* (Gmelin)) in California and Italy. Clim Change 95:195–217. https://doi.org/10.1007/s10584-008-9528-4
11. Ponti L, Gutierrez AP, Giannakopoulos C et al (2024) Prospective regional analysis of olive and olive fly in Andalusia under climate change using physiologically based demographic modeling powered by cloud computing. Clim Serv 34:100455. https://doi.org/10.1016/j.cliser.2024.100455
12. Ponti L, Gutierrez AP, Neteler M (2024) GRASS GIS database for CASAS-PBDM (www.casasglobal.org) geospatial mapping and analysis
13. Gutierrez AP, Ponti L (2013) Deconstructing the control of the spotted alfalfa aphid *Therioaphis maculata*. Agric For Entomol 15:272–284. https://doi.org/10.1111/afe.12015
14. Gilbert N, Gutierrez AP, Frazer BD, Jones RE (1976) Ecological relationships. W.H. Freeman and Co, Reading and San Francisco
15. Gutierrez AP (1992) The physiological basis of ratio-dependent predator-prey theory: the metabolic pool model as a paradigm. Ecology 73:1552–1563. https://doi.org/10.2307/1940008
16. Gutierrez AP, Mills NJ, Schreiber SJ, Ellis CK (1994) A physiologically based tritrophic perspective on bottom-up-top-down regulation of populations. Ecology 75:2227–2242. https://doi.org/10.2307/1940879
17. Mills NJ, Gutierrez AP (1999) Biological control of insect pest: a tritrophic perspective. In: Hawkins BA, Cornell VH (eds) Theoretical approaches to biological control. Cambridge University Press, Cambridge, pp 89–102
18. Hughes RD, Gilbert N (1968) A model of an aphid population—a general statement. J Anim Ecol 37:553–563. https://doi.org/10.2307/3074
19. Gilbert N, Gutierrez AP (1973) A plant-aphid-parasite relationship. J Anim Ecol 42:323–340. https://doi.org/10.2307/3288
20. Cure JR, Rodríguez D, Gutierrez AP, Ponti L (2020) The coffee agroecosystem: bio-economic analysis of coffee berry borer control (*Hypothenemus hampei*). Sci Rep 10:12262. https://doi.org/10.1038/s41598-020-68989-x
21. Gutierrez AP, Ponti L, Kranthi KR et al (2020) Bio-economics of Indian hybrid Bt cotton and farmer suicides. Environ Sci Eur 32:139. https://doi.org/10.1186/s12302-020-00406-6
22. Gutierrez AP, Kenmore PE, Ponti L (2023) Hybrid Bt cotton is failing in India: cautions for Africa. Environ Sci Eur 35:93. https://doi.org/10.1186/s12302-023-00804-6
23. Regev U, Gutierrez AP, Schreiber SJ, Zilberman D (1998) Biological and economic foundations of renewable resource exploitation. Ecol Econ 26:227–242. https://doi.org/10.1016/S0921-8009(97)00103-1
24. Pemsl DE, Gutierrez AP, Waibel H (2008) The economics of biotechnology under ecosystem disruption. Ecol Econ 66:177–183. https://doi.org/10.1016/j.ecolecon.2007.08.022
25. Baumgärtner J (2022) Postmodern agriculture and rural development: unfolding and fading research themes on the voyage to a sustainable future: essay with personal annotations, 1st edn. Deutscher Wissenschafts-Verlag (DWV), Baden-Baden, Auflage
26. Gutierrez AP, Schulthess F, Wilson LT et al (1987) Energy acquisition and allocation in plants and insects: a hypothesis for the possible role of hormones in insect feeding patterns. Can Entomol 119:109–129. https://doi.org/10.4039/Ent119109-2
27. de Wit CT, Goudriaan J (1978) Simulation of ecological processes. PUDOC, Wageningen
28. Gutierrez AP, Falcon LA, Loew W et al (1975) An analysis of cotton production in California: a model for Acala cotton and the effects of defoliators on its yields. Environ Entomol 4:125–136. https://doi.org/10.1093/ee/4.1.125
29. Wang Y, Gutierrez AP, Oster G, Daxl R (1977) A population model for plant growth and development: coupling cotton-herbivore interaction. Can Entomol 109:1359–1374. https://doi.org/10.4039/Ent1091359-10
30. Gutierrez AP, Yaninek JS, Neuenschwander P, Ellis CK (1999) A physiologically based tritrophic metapopulation model of the African cassava food web. Ecol Model 123:225–242. https://doi.org/10.1016/S0304-3800(99)00144-1
31. Messenger PS (1964) Use of lifetables in a bioclimatic study of an experimental aphid-braconid wasp host-parasite system. Ecology 45:119–131
32. de Candolle A (1855) Géographie botanique raisonnée. Librairie de Victor Masson, Paris
33. Briére JF, Pracros P, Le Roux AY, Pierre JS (1999) A novel rate model of temperature-dependent development for arthropods. Environ Entomol 28:22–29. https://doi.org/10.1093/ee/28.1.22
34. Frazer BD, Gilbert N (1976) Coccinellids and aphids: a quantitative study of the impact of adult ladybirds (Coleoptera: Coccinellidae) preying on field populations of pea aphids (Homoptera: Aphididae). J Entomol Soc B C 73:33–56
35. Ritchie JT, Gerakis A, Suleiman A (1999) Simple model to estimate field-measured soil water limits. Trans ASAE 42:1609–1614
36. von Arx R, Baumgärtner J, Delucchi V (1983) A model to simulate the population-dynamics of *Bemisia tabaci* Genn. (Stern., Aleyrodidae) on cotton in the Sudan Gezira. Zeitschrift für Angewandte Entomol 96:341–363. https://doi.org/10.1111/j.1439-0418.1983.tb03681.x
37. Grossiord C, Buckley TN, Cernusak LA et al (2020) Plant responses to rising vapor pressure deficit. New Phytol 226:1550–1566. https://doi.org/10.1111/nph.16485
38. von Liebig J (1840) Chemistry and its applications to agriculture and physiology. Taylor and Walton, London
39. Gutierrez AP, Butler GD Jr, Ellis CK (1981) Pink bollworm: diapause induction and termination in relation to fluctuating temperatures and decreasing photophases. Environ Entomol 10:936–942
40. Johnsen S, Gutierrez AP, Jorgensen J (1997) Overwintering in the cabbage root fly *Delia radicum*: a dynamic model of temperature-dependent dormancy and post-dormancy development. J Appl Ecol 34:21–28. https://doi.org/10.2307/2404844
41. Di Cola G, Gilioli G, Baumgärtner J (1999) Mathematical models for age-structured population dynamics. In: Huffaker CB, Gutierrez AP (eds) Ecological entomology, 2nd edn. Wiley, New York
42. Buffoni G, Pasquali S (2007) Structured population dynamics: continuous size and discontinuous stage structures. J Math Biol 54:555–595. https://doi.org/10.1007/s00285-006-0058-2
43. Abkin MH, Wolf C (1976) Computer library for agricultural systems simulation. Distributed delay routines: DEL, DELS, DELF, DELLF, DELVF, DELLVF. Department of Agricultural Economics, Michigan State University, Lansing, MI, USA
44. Manetsch TJ (1976) Time-varying distributed delays and their use in aggregative models of large systems. IEEE Trans Syst Man Cybern 6:547–553. https://doi.org/10.1109/TSMC.1976.4309549
45. Vansickle J (1977) Attrition in distributed delay models. IEEE T Syst Man Cyb 7:635–638. https://doi.org/10.1109/TSMC.1977.4309800
46. Severini M, Alilla R, Pesolillo S, Baumgärtner J (2005) Fenologia della vite e della *Lobesia botrana* (Lep. Tortricidae) nella zona dei Castelli Romani. Rivista Ital di Agrometeorol 3:34–39
47. Stone ND, Gutierrez AP (1986) A field-oriented simulation of pink bollworm in southwestern desert cotton. Hilgardia 54:1–24
48. Wang YH, Gutierrez AP (1980) An assessment of the use of stability analyses in population ecology. J Anim Ecol 49:435–452. https://doi.org/10.2307/4256
49. Ponti L, Gutierrez AP, de Campos MR et al (2021) Biological invasion risk assessment of *Tuta absoluta*: mechanistic versus correlative methods. Biol Invasions 23:3809–3829. https://doi.org/10.1007/s10530-021-02613-5

50. Ruane AC, Goldberg R, Chryssanthacopoulos J (2015) Climate forcing datasets for agricultural modeling: Merged products for gap-filling and historical climate series estimation. Agric For Meteorol 200:233–248. https://doi.org/10.1016/j.agrformet.2014.09.016
51. GRASS Development Team (2022) Geographic Resources Analysis Support System (GRASS) Software, Version 8.2.0. Open Source Geospatial Foundation. Beaverton, Oregon, USA. http://grass.osgeo.org
52. Neteler M, Bowman MH, Landa M, Metz M (2012) GRASS GIS: a multi-purpose open source GIS. Environ Model Softw 31:124–130. https://doi.org/10.1016/j.envsoft.2011.11.014
53. Gutierrez AP, Ponti L (2014) The new world screwworm: prospective distribution and role of weather in eradication. Agric For Entomol 16:158–173. https://doi.org/10.1111/afe.12046
54. Gutierrez AP, Ponti L, Arias PA (2019) Deconstructing the eradication of new world screwworm in North America: retrospective analysis and climate warming effects. Med Vet Entomol 33:282–295. https://doi.org/10.1111/mve.12362
55. Vargas-Terán M, Hofmann H, Tweddle N (2005) Impact of screwworm eradication programmes using the sterile insect technique. In: Dyck VA, Hendrichs J, Robinson AS (eds) Sterile insect technique. Principles and practice in area-wide integrated pest management. Springer, Berlin, pp 629–650
56. El-Azazy OME (1992) Observations of the new world screwworm fly in Libya and the risk of its entrance into Egypt. Vet Parasitol 42:303–310. https://doi.org/10.1016/0304-4017(92)90072-H
57. Besnard G, Khadari B, Navascués M et al (2013) The complex history of the olive tree: from Late Quaternary diversification of Mediterranean lineages to primary domestication in the northern Levant. Proc Royal Soc London B Biol Sci 280:20122833. https://doi.org/10.1098/rspb.2012.2833
58. Bongi G (2002) Freezing avoidance in olive tree (*Olea europaea* L.): from proxies to targets of action. Adv Hortic Sci 16:117–124
59. Fiorino P (2003) Olea: trattato di olivicoltura. Edagricole, Bologna
60. Vitagliano C, Sebastiani L (2002) Physiological and biochemical remarks on environmental stress in olive (*Olea europaea* L.). Acta Hortic 586:435–440. https://doi.org/10.17660/ActaHortic.2002.586.89
61. Ponti L, Gutierrez AP, Ruti PM, Dell'Aquila A (2014) Fine-scale ecological and economic assessment of climate change on olive in the Mediterranean Basin reveals winners and losers. Proc Natl Acad Sci USA 111:5598–5603. https://doi.org/10.1073/pnas.1314437111
62. Fernandez JE, Moreno F (1999) Water use by the olive tree. J Crop Prod 2:101–162
63. Gutierrez AP, Sabbatini-Peverieri G, Ponti L et al (2023) Tritrophic analysis of the prospective biological control of brown marmorated stink bug, *Halyomorpha halys*, under extant weather and climate change. J Pest Sci. https://doi.org/10.1007/s10340-023-01610-y
64. Yonow T, Kriticos DJ, Ota N et al (2021) Modelling the potential geographic distribution of two *Trissolcus* species for the brown marmorated stink bug. Halyomorpha Halys Insects 12:491. https://doi.org/10.3390/insects12060491
65. Sutherst RW, Maywald GF (1985) A computerised system for matching climates in ecology. Agr Ecosyst Environ 13:281–299. https://doi.org/10.1016/0167-8809(85)90016-7
66. Tang FHM, Nguyen TH, Conchedda G et al (2024) CROPGRIDS: a global geo-referenced dataset of 173 crops. Sci Data 11:413. https://doi.org/10.1038/s41597-024-03247-7
67. Campos MR, Béarez P, Amiens-Desneux E et al (2021) Thermal biology of *Tuta absoluta*: demographic parameters and facultative diapause. J Pest Sci 94:829–842. https://doi.org/10.1007/s10340-020-01286-8
68. Van Damme V, Berkvens N, Moerkens R et al (2015) Overwintering potential of the invasive leafminer *Tuta absoluta* (Meyrick) (Lepidoptera: Gelechiidae) as a pest in greenhouse tomato production in Western Europe. J Pest Sci 88:533–541. https://doi.org/10.1007/s10340-014-0636-9
69. da Krechemer FS, Foerster LA (2015) *Tuta absoluta* (Lepidoptera: Gelechiidae): Thermal requirements and effect of temperature on development, survival, reproduction and longevity. Eur J Entomol. https://doi.org/10.14411/eje.2015.103
70. Martins JC, Picanço MC, Bacci L et al (2016) Life table determination of thermal requirements of the tomato borer *Tuta absoluta*. J Pest Sci. https://doi.org/10.1007/s10340-016-0729-8.10.1007/s10340-016-0729-8
71. Kahrer A, Moyses A, Hochfellner L et al (2019) Modelling time-varying low-temperature induced mortality rates for pupae of *Tuta absoluta* (Gelechiidae, Lepidoptera). J Appl Entomol. https://doi.org/10.1111/jen.12693
72. EFSA Plh Panel (EFSA Panel on Plant Health), Bragard C, Baptista P et al (2023) Assessment of the probability of introduction of *Thaumatotibia leucotreta* into the European Union with import of cut roses. EFSA J 21:e08107. https://doi.org/10.2903/j.efsa.2023.8107
73. Daiber CC (1979) A study of the biology of the false codling moth [*Cryptophlebia leucotreta* (Meyr.)]: the larva. Phytophylactica 11:141–144. https://doi.org/10.10520/AJA03701263_526
74. Daiber CC (1979) A study of the biology of the false codling moth [*Cryptophlebia leucotreta* (Meyr.)]: the egg. Phytophylactica 11:129–132. https://doi.org/10.10520/AJA03701263_523
75. Daiber CC (1979) A study of the biology of the false codling moth [*Cryptophlebia leucotreta* (Meyr.)]: the cocoon. Phytophylactica 11:151–157. https://doi.org/10.10520/AJA03701263_496
76. Daiber CC (1980) A study of the biology of the false codling moth *Cryptophlebia leucotreta* (Meyr.): the adult and generations during the year. Phytophylactica 12:187–194. https://doi.org/10.10520/AJA03701263_482
77. Terblanche JS, Mitchell KA, Uys W et al (2017) Thermal limits to survival and activity in two life stages of false codling moth *Thaumatotibia leucotreta* (Lepidoptera, Tortricidae). Physiol Entomol 42:379–388. https://doi.org/10.1111/phen.12210
78. Goergen G, Kumar PL, Sankung SB et al (2016) First report of outbreaks of the fall armyworm *Spodoptera frugiperda* (J E Smith) (Lepidoptera, Noctuidae), a new alien invasive pest in West and Central Africa. PLoS ONE 11:e0165632. https://doi.org/10.1371/journal.pone.0165632
79. Overton K, Maino JL, Day R et al (2021) Global crop impacts, yield losses and action thresholds for fall armyworm (*Spodoptera frugiperda*): a review. Crop Prot 145:105641. https://doi.org/10.1016/j.cropro.2021.105641
80. Barfield CS, Mitchell ER, Poeb SL (1978) A temperature-dependent model for fall armyworm development. Ann Entomol Soc Am 71:70–74. https://doi.org/10.1093/aesa/71.1.70
81. Ali A, Luttrell RG, Schneider JC (1990) Effects of temperature and larval diet on development of the fall armyworm (Lepidoptera: Noctuidae). Ann Entomol Soc Am 83:725–733. https://doi.org/10.1093/aesa/83.4.725
82. Gilioli G, Colli P, Colturato M et al (2021) A nonlinear model for stage-structured population dynamics with nonlocal density-dependent regulation: an application to the fall armyworm moth. Math Biosci. https://doi.org/10.1016/j.mbs.2021.108573
83. Gilioli G, Sperandio G, Simonetto A et al (2022) Assessing the risk of establishment and transient populations of *Spodoptera frugiperda* in Europe. J Pest Sci. https://doi.org/10.1007/s10340-022-01517-0
84. Gutierrez AP, Adamczyk JJ, Ponsard S, Ellis CK (2006) Physiologically based demographics of Bt cotton–pest interactions II. Temporal refuges, natural enemy interactions. Ecol Model 191:360–382. https://doi.org/10.1016/j.ecolmodel.2005.06.002
85. Shivankar V, Rao C, Singh S (2000) Studies on citrus psylla, *Diaphorina citri* Kuwayama: a review. Agric Rev 21:199–204
86. Halbert SE, Manjunath KL (2004) Asian citrus psyllids (Sternorrhyncha: Psyllidae) and greening disease of citrus: a literature review and assessment of risk in Florida. Flen 87:330–353
87. Etienne J, Aubert B (1980) Biological control of psyllid vectors of greening disease on Reunion Island. Int Organ Citrus Virol Conf Proc 1957–2010:8. https://doi.org/10.5070/C55V15K79K
88. Halbert SE, Núñez CA (2004) Distribution of the Asian citrus psyllid, *Diaphorina citri* Kuwayama (Rhynchota: Psyllidae) in the Caribbean Basin. Flen 87:401–402
89. Halbert S (1999) Asian citrus psyllid - A serious exotic pest of FL citrus. Pest Alert FDACS-P-01646, Florida Department of Agriculture and Consumer Services, Division of Plant Industry https://ccmedia.fdacs.gov/content/download/68181/file/Pest_Alert_-_Diaphorina_citri_Asian_citrus_psyllid.pdf. Accessed 9 Sep 2024
90. Etienne J, Quilici S, Marival D, Franck A (2001) Biological control of *Diaphorina citri* (Hemiptera: Psyllidae) in Guadeloupe by imported

Tamarixia radiata (Hymenoptera: Eulophidae). Fruits 56:307–315. https://doi.org/10.1051/fruits:2001131
91. French JV, Kahlke C, da Graça JV (2001) First record of the Asian citrus psylla, *Diaphorina citri* Kuwayama (Homoptera: Psyllidae) in Texas. Subtro Plant Sci 53:14–15
92. Grafton-Cardwell EE, Stelinski LL, Stansly PA (2013) Biology and management of Asian citrus psyllid, vector of the Huanglongbing pathogens. Annu Rev Entomol 58:413–432. https://doi.org/10.1146/annurev-ento-120811-153542
93. Grafton-Cardwell E, Daugherty M (2018) UC IPM Pest Notes: Asian citrus psyllid and huanglongbing disease. University of California, Division of Agriculture & Natural Resources (UC ANR) Publication 74155. https://anrcatalog.ucanr.edu/Details.aspx?itemNo=74155. Accessed 22 July 2023
94. Aidoo OF, Tanga CM, Mohamed SA et al (2020) Detection and monitoring of 'Candidatus' Liberibacter spp. vectors: African citrus triozid *Trioza erytreae* Del Guercio (Hemiptera: Triozidae) and Asian citrus psyllid *Diaphorina citri* Kuwayama (Hemiptera: Liviidae) in citrus groves in East Africa. Agric For Entomol 22:401–409. https://doi.org/10.1111/afe.12395
95. Aubert B (2011) A new threat to Mediterranean citrus. FruiTrop 168:4–9
96. Godefroid M (2023) Species distribution models predicting climate suitability for the psyllid *Trioza erytreae*, vector of citrus greening disease. Crop Prot 168:106228. https://doi.org/10.1016/j.cropro.2023.106228
97. Gutierrez AP, Ponti L (2013) Prospective analysis of the geographic distribution and relative abundance of Asian citrus psyllid (Hemiptera: Liviidae) and citrus greening disease in North America and the Mediterranean Basin. Fla Entomol 96:1375–1391. https://doi.org/10.1653/024.096.0417
98. Coletta-Filho HD, Targon MLPN, Takita MA et al (2004) First report of the causal agent of huanglongbing ("candidatus liberibacter asiaticus") in brazil. Plant Dis 88:1382–1382. https://doi.org/10.1094/PDIS.2004.88.12.1382C
99. Halbert SE (2005) Citrus greening/Huanglongbing. Pest Alert, Florida Department of Agriculture and Consumer Services, Division of Plant Industry, Gainesville, Florida. http://web.science.oregonstate.edu/bpp/Plant_Clinic/Disease_sheets/Citrus%20Greening%20pest%20alert.pdf. Accessed 3 Mar 2025
100. Bar-Zeev M (1957) The effect of extreme temperatures on different stages of *Aëdes aegypti* (L.). Bull Entomol Res 48:593–599. https://doi.org/10.1017/S0007485300002765
101. Bar-Zeev M (1958) The effect of temperature on the growth rate and survival of the immature stages of *Aëdes aegypti* (L.). Bull Entomol Res 49:157–163. https://doi.org/10.1017/S0007485300053499
102. Delatte H, Dehecq JS, Thiria J et al (2008) Geographic distribution and developmental sites of *Aedes albopictus* (Diptera: Culicidae) during a Chikungunya epidemic event. Vector-Borne Zoonotic Dis 8:25–34. https://doi.org/10.1089/vbz.2007.0649
103. Delatte H, Gimonneau G, Triboire A, Fontenille D (2009) Influence of temperature on immature development, survival, longevity, fecundity, and gonotrophic cycles of *Aedes albopictus*, vector of chikungunya and dengue in the Indian Ocean. J Med Entomol 46:33–41
104. Brady OJ, Johansson MA, Guerra CA et al (2013) Modelling adult *Aedes aegypti* and *Aedes albopictus* survival at different temperatures in laboratory and field settings. Prasites Vectors 8:9
105. Brady OJ, Golding N, Pigott DM et al (2014) Global temperature constraints on Aedes aegypti and Ae. albopictus persistence and competence for dengue virus transmission. Parasites Vectors 7:338
106. Carrington LB, Armijos MV, Lambrechts L, Scott TW (2013) Fluctuations at a low mean temperature accelerate dengue virus transmission by *Aedes aegypti*. PLoS Negl Trop Dis 7:e2190. https://doi.org/10.1371/journal.pntd.0002190
107. Eisen L, Monaghan AJ, Lozano-Fuentes S et al (2014) The impact of temperature on the bionomics of *Aedes (Stegomyia) aegypti*, with special reference to the cool geographic range margins. J Med Entomol 51:496–516. https://doi.org/10.1603/ME13214
108. Jia P, Lu L, Chen X et al (2016) A climate-driven mechanistic population model of *Aedes albopictus* with diapause. Parasites Vectors 9:175. https://doi.org/10.1186/s13071-016-1448-y
109. Perez MH, Noriega FG (2013) *Aedes aegypti* pharate 1st instar quiescence: a case for anticipatory reproductive plasticity. J Insect Physiol 59:318–324. https://doi.org/10.1016/j.jinsphys.2012.12.007
110. Denlinger DL, Armbruster PA (2014) Mosquito diapause. Annu Rev Entomol 59:73–93. https://doi.org/10.1146/annurev-ento-011613-162023
111. Diniz DFA, De Albuquerque CMR, Oliva LO et al (2017) Diapause and quiescence: dormancy mechanisms that contribute to the geographical expansion of mosquitoes and their evolutionary success. Parasites Vectors 10:310. https://doi.org/10.1186/s13071-017-2235-0
112. Oliva L, La Corte R, Santana M, Albuquerque C (2018) Quiescence in *Aedes aegypti*: interpopulation differences contribute to population dynamics and vectorial capacity. Insects 9:111. https://doi.org/10.3390/insects9030111
113. Armbruster PA (2016) Photoperiodic diapause and the establishment of *Aedes albopictus* (Diptera: Culicidae) in North america. J Med Entomol 53:1013–1023. https://doi.org/10.1093/jme/tjw037
114. Batz ZA, Armbruster PA (2018) Diapause-associated changes in the lipid and metabolite profile of the Asian tiger mosquito *Aedes albopictus*. J Exp Biol Jeb. https://doi.org/10.1242/jeb.189480
115. Westby KM, Medley KA (2020) Cold nights, city lights: artificial light at night reduces photoperiodically induced diapause in urban and rural populations of *Aedes albopictus* (Diptera: Culicidae). J Med Entomol 57:1694–1699. https://doi.org/10.1093/jme/tjaa139
116. Hand SC, Podrabsky JE (2000) Bioenergetics of diapause and quiescence in aquatic animals. Thermochim Acta 349:31–42. https://doi.org/10.1016/S0040-6031(99)00511-0
117. Perez MH, Noriega FG (2012) *Aedes aegypti* pharate 1st instar quiescence affects larval fitness and metal tolerance. J Insect Physiol 58:824–829. https://doi.org/10.1016/j.jinsphys.2012.03.005
118. Kraemer MU, Sinka ME, Duda KA et al (2015) The global distribution of the arbovirus vectors *Aedes aegypti* and *Ae. albopictus*. Elife 4:e08347. https://doi.org/10.7554/eLife.08347
119. Pasquali S, Mariani L, Calvitti M et al (2020) Development and calibration of a model for the potential establishment and impact of *Aedes albopictus* in Europe. Acta Trop 202:105228. https://doi.org/10.1016/j.actatropica.2019.105228
120. Calvitti M, Moretti R, Lampazzi E et al (2010) Characterization of a new *Aedes albopictus* (Diptera: Culicidae)-*Wolbachia pipientis* (Rickettsiales: Rickettsiaceae) symbiotic association generated by artificial transfer of the *w*Pip strain from *Culex pipiens* (Diptera: Culicidae). J Med Entomol 47:179–187
121. Gutierrez AP, Ponti L, Neteler M et al (2021) Invasive potential of tropical fruit flies in temperate regions under climate change. Commun Biol 4:1–14. https://doi.org/10.1038/s42003-021-02599-9
122. Teets NM, Hahn DA (2018) Genetic variation in the shape of cold-survival curves in a single fly population suggests potential for selection from climate variability. J Evol Biol 31:543–555. https://doi.org/10.1111/jeb.13244
123. Gutierrez AP, Ponti L, Dalton DT (2016) Analysis of the invasiveness of spotted wing Drosophila (*Drosophila suzukii*) in North America, Europe, and the Mediterranean Basin. Biol Invasions 18:3647–3663. https://doi.org/10.1007/s10530-016-1255-6
124. Hawkins BA, Cornell HV (1999) Theoretical approaches to biological control. Cambridge University Press, Cambridge
125. Ponti L, Gilioli G, Biondi A et al (2015) Physiologically based demographic models streamline identification and collection of data in evidence-based pest risk assessment. EPPO Bull 45:317–322. https://doi.org/10.1111/epp.12224
126. Gutierrez AP, Ponti L, Levi-Mourao A et al (in press) Stabilizing adaptation in an invasive species: alfalfa weevil as a case study. Agricultural and Forest Entomology
127. Schreiber SJ, Gutierrez AP (1998) A supply/demand perspective of species invasions and coexistence: applications to biological control. Ecol Model 106:27–45. https://doi.org/10.1016/S0304-3800(97)00178-6

Publisher's Note